AFOSR-TR- 81-0892

AD A110183

SGI-R-81-048

RELATIVE WAVEFORM INVERSION

LEVEL II

G.R. MELLMAN

S.K. KAUFMAN

DTIC
ELECTE
JAN 28 1982
S D
E

SEMI-ANNUAL TECHNICAL REPORT
FOR PERIOD ENDING APRIL 30, 1981

SPONSORED BY

ADVANCED RESEARCH PROJECTS AGENCY (DOD)

ARPA ORDER NO. 3291-40

MONITORED BY AFOSR UNDER CONTRACT #F49620-81-C-0025

DTIC FILE COPY

The views and conclusions contained in this document are those of the authors and should not be interpreted as necessarily representing the official policies, either expressed or implied, of the Defense Advanced Research Projects Agency or the United States Government.

This document has been approved for public release and sale; its distribution is unlimited.

82 01 28 028

SIERRA GEOPHYSICS

15446 BELL-RED ROAD, SUITE 400 • REDMOND, WASHINGTON 98052 • (206) 881-8833

Approved for public release;
distribution unlimited.

ARPA Order No. 3291-40

Program Code: 1A10

Effective date of Contract: November 1, 1980

Contract Expiration Date: October 31, 1982

Amount of Contract: $567,447

Principal Investigators and Phone No.:

Dr. G. M. Lundquist

Dr. D. M. Hadley

(206) 881-8833

Program Manager and Phone No.:

Mr. William J. Best

(202) 767-4908

SGI-R-81-048

RELATIVE WAVEFORM INVERSION

G.R. MELLMAN

S.K. KAUFMAN

SEMI-ANNUAL TECHNICAL REPORT

FOR PERIOD ENDING APRIL 30, 1981

SPONSORED BY

ADVANCED RESEARCH PROJECTS AGENCY (DOD)

ARPA ORDER NO. 3291-~~40~~

MONITORED BY AFOSR UNDER CONTRACT #F49620-81-C-0025

The views and conclusions contained in this document are those of the authors and should not be interpreted as necessarily representing the official policies, either expressed or implied, of the Defense Advanced Research Projects Agency or the United States Government.

AIR FORCE OFFICE OF SCIENTIFIC RESEARCH (AFSC)
NOTICE OF TRANSMITTAL TO DTIC
This technical report has been reviewed and is
approved for public release IAW AFR 190-12.
Distribution is unlimited.
MATTHEW J. KERPER
Chief, Technical Information Division

Unclassified

SECURITY CLASSIFICATION OF THIS PAGE (When Data Entered)

REPORT DOCUMENTATION PAGE

READ INSTRUCTIONS BEFORE COMPLETING FORM

1. REPORT NUMBER: AFOSR-TR- 81-0892
2. GOVT ACCESSION NO.: AD-A110183
3. RECIPIENT'S CATALOG NUMBER:
4. TITLE (and Subtitle): Relative Waveform Inversion
5. TYPE OF REPORT & PERIOD COVERED: Semi-Annual Technical Report Nov. 1, 1980-Apr 30, 1981
6. PERFORMING ORG. REPORT NUMBER: SGI-R-81-048
7. AUTHOR(s): Dr. G.R. Mellman, S.K. Kaufman
8. CONTRACT OR GRANT NUMBER(s): F49260-81-C-0025
9. PERFORMING ORGANIZATION NAME AND ADDRESS: Sierra Geophysics, Inc., 15446 Bell-Red Rd., Suite 400, Redmond, WA 98052
10. PROGRAM ELEMENT, PROJECT, TASK AREA & WORK UNIT NUMBERS: 61102F, 2309/A1
11. CONTROLLING OFFICE NAME AND ADDRESS: Air Force Office of Scientific Research, Building 410, Bolling AFB, Washington, DC 20332
12. REPORT DATE: November 1981
13. NUMBER OF PAGES: 72
14. MONITORING AGENCY NAME & ADDRESS (if different from Controlling Office):
15. SECURITY CLASS. (of this report): Unclassified
15a. DECLASSIFICATION/DOWNGRADING SCHEDULE:
16. DISTRIBUTION STATEMENT (of this Report): Approved For Public Release; Distribution unlimited
17. DISTRIBUTION STATEMENT (of the abstract entered in Block 20, if different from Report):
18. SUPPLEMENTARY NOTES:
19. KEY WORDS (Continue on reverse side if necessary and identify by block number):
Body waves
Inversion
Waveforms
Underground Explosions

20. ABSTRACT (Continue on reverse side if necessary and identify by block number):

A relative waveform inversion method has been developed which determines models that correctly predict waveform changes in a set of observed seismograms. By modeling changes in waveforms rather than absolute waveforms, a number of relatively poorly determined quantities, such as receiver function and Q, may be eliminated from the problem and greater resolution of key model parameters obtained. The method has been applied to the estimation of overall amplitude, pP amplitude and pP delay time for a suite of

DD FORM 1 JAN 73 1473A EDITION OF 1 NOV 65 IS OBSOLETE

Unclassified

SECURITY CLASSIFICATION OF THIS PAGE (When Data Entered)

393821

seven presumed underground nuclear explosions in the Eastern Kazakh region. Events divide into two populations based on pP amplitude, with events having small pP amplitude possibly showing indications of azimuthal variation in pP. The existence of events with radically different pP amplitudes suggests that biases may exist in current relative yield estimation techniques, an effect which is corrected for in the relative waveform method.

Accession For
NTIS GRA&I ☒
DTIC TAB ☐
Unannounced ☐
Justification
By
Distribution/
Availability Codes
Dist | Avail and/or Special
A
COPY INSPECTED 3

TABLE OF CONTENTS

Title	Page
I. INTRODUCTION	2
II. RELATIVE WAVEFORM INVERSION	6
III. SYNTHETIC RESULTS	17
IV. APPLICATION TO DATA	48
V. CONCLUSIONS	69
REFERENCES	70
APPENDIX	71

I. INTRODUCTION

Two basic classes of methods have generally been used in the analysis of seismic data. The older, and still most prevalently used, class of methods we will call data parametrization methods. The other, more recently developed class of methods, we will call modeling methods.

Data parametrization methods are those techniques in which we attempt to find models that fit only selected aspects of the data. That is, a parametrization of the data is chosen which does not completely describe the data, and these parameters are then used to determine suitable models. Examples of such parametrizations include travel times, spectral slopes and power spectra. While these features of the data may contain much of the information concerning the model parameter of interest, they are not, in themselves, sufficient to completely recover the data.

In modeling studies, on the other hand, no parametrization of the data is used, although data may be prefiltered and windowed. Instead, we attempt to construct best fitting estimates of the prefiltered data, using estimates of all necessary model parameters.

The major advantage of data parametrization methods is that it is often possible to find simple functional forms relating the parametrized data to the parametrized model. This allows the inverse problem to be done quite simply, often as a simple linear, least squares problem even when no such simple solution of the full inverse problem exists.

PRECEDING PAGE BLANK-NOT FILMED

A second advantage is the ease with which relative variations in a single model parameter may be studied. A variety of spectral ratio and similar techniques are available which allow a single or small number of model parameters to be isolated and variations in these data characteristics to completely define the model studied independently of other factors necessary.

The principal advantage of modeling studies, on the other hand, is the greater resolution that can often be obtained by making use of non-parametrized data seismograms. One example of this approach is the fine structure obtained through waveform inversion of triplication data, compared to the models obtainable through more standard travel-time analysis (Mellman, 1980).

Use of the additional data in the non-parametrized seismogram means that it is always possible to find a modeling method that gives greater model resolution, or smaller model variance, than is obtainable in a corresponding data parametrization study. Unfortunately, it is often not possible to achieve that resolution in practice. Such results can only be achieved through the proper choice of error function, a fact which is ignored in most model studies. Indeed, most forward modeling studies rely on fitting by eye, rather than on optimization of an error function. While this gives the researcher considerable flexibility in choice of which aspects of the data are important, it is difficult to assess how well the model is constrained.

During the course of a study, one usually achieves a strong intuitive feel for model constraint, but it is virtually impossible to pass this intuition on to others in the field. Moreover, due to the existence of unrecognized tradeoffs, this intuitive feel for the model constraints may be misleading or incorrect.

The use of formal inverse methods in modeling studies requires the adoption of an objective error function. Even in this approach, however, little attention is paid to choosing error functions that provide the best constrained models. Proper choice of these error functions is intimately related to effects of various types of noise on the final solution. This includes both modeling noise, which is almost universally ignored, and the more commonly considered data noise. This topic is relatively poorly understood, and much additional work is necessary, paritcularly for nonlinear problems.

Even without optimal choice of an error function, modeling studies can often indicate the presence of noise problems in cases where data parametrization methods give no indication of any problems. This is especially true in the case of modeling noise. By modeling noise, we mean noise induced by incomplete or incorrect model parametrization. It is often only by detailed analysis of data misfits in modeling studies that it is possible to decide that a more general model is appropriate. This can effect not only estimates of the model, but estimates of the uncertainty of model parameters as well.

A major disadvantage of modeling studies has been the absence of a stable, generally applicable modeling method equivalent to spectral ratio methods for the study of relative changes of a suite of seismograms. Such methods do exist for specific cases, such as attenuation studies (Burdick and Helmberger, 1974) where group properties of the attenuation operator may be exploited to provide stable estimates of differential attenuation. In general, however, the only method available for relative studies has been deconvolution, which is notorious for its instability under even the best of circumstances.

What criteria would we like in a relative modeling method? First, we require the method to be symmetric with respect to the data. That is, the results should be inpendent of the designation of any particular datum as the reference datum. Thus no datum is given a preferred position in the method. Second, the method should be stable. Third, we would like to have sufficient local linearity to make an iterative linearized inversion procedure feasible. We note that deconvolution methods satisfy none of these criteria. In the following section, we describe a method that does satisfy these criteria and its inverse as applied to seismic waveform data. We will call this method relative waveform inversion.

II. RELATIVE WAVEFORM INVERSION

Consider two seismograms, $f_1(t)$ and $f_2(t)$ composed of a common transfer function $T(t)$ and a portion $S_i(t)$ which differs from seismogram to seismogram. If we choose $f_1(t)$ and $f_2(t)$ to be seismograms rcorded at a single station in the far field for two events in a common source region then the transfer function T would contain instrument, path, and surce properties, and receiver response functions common to both seismograms. The remaining source and propagation terms are included in S_i. Then, by definition

$$f_i(t) \equiv T(t) * S_i(t) \tag{1}$$

If this expression is exact, then

$$f_1(t) * S_2(t) = f_2(t) * S_1(t) \tag{2}$$

This suggests that minimization of the error functional

$$\begin{aligned} e_{12} &= \| F_{12}(t) \|_W \qquad \text{where} \\ F_{12}(t) &= f_1 * S_2 - f_2 * S_1 \qquad \text{and} \\ \| X(t) \|_W &= \int | X(t) * W(t) |^2 dt. \end{aligned} \tag{3}$$

will provide a good estimate of the functions S_i.

The weighting function W acts as a prewhitening filter and is chosed to extend the usable signal bandwidth while still rejecting noise. In general, choice of W will depend

on the frequency content of f_i and S_i and on the noise spectra. For the applications discussed below, simple functions of the form $W(\omega) = (1+k\omega)$ were found to be adequate. Choice of the error function $F_{12}(t)$ in equation 3 leads to a relative waveform method that satisfies the three criteria presented in the introduction. The error functional e_{12} is invarient to interchange of indicies, assuring that neither seismogram occupies a preferred position. Further, the error function F_{12} consists of differences of the convolutions of well-behaved functions which assures stability. While the local linearity of F_{12} with respect to model parameters depends on the choice of model parametrization, the functional form of F_{12} gives promise of sufficient linearity for a wide variety of model parameterization to make iterative linearized inversion feasable.

The error functional e_{12} in equation 2 may be readily extended to multiple recording stations. Let e^i_{12} be the error functional for the ith station with f_{ji} the seismogram for event j at station i. We may then define a new error functional.

$$(e_{12})^2 = \Sigma\ V_i^2 (e^i_{12})^2 \qquad (4)$$

$$\text{with} \quad V_i = \left(\int f^2_{1i}(t)dt\right)^{-\frac{1}{2}} \left(\int f^2_{2i}(t)dt\right)^{-\frac{1}{2}}$$

Here V_i is a station weighting factor, used to prevent high amplitude observations from dominating the solution.

One obvious application of the relative waveform inversion technique is the estimation of "depth corrections" to the yields of underground nuclear explosions. It has been appreciated for some time that surface reflections have a major effect on both waveform and amplitude of shallow events. Efforts to account for thses effects have often taken form of modeling studies, where elastic wave velocities are used to predict arrival times and amplitudes of surface reflections. See, for example, Burdick and Helmberger (1979). Such approaches have been criticized for the linear assumptions used in what is clearly a nonlinear regime. In particular, it is often observed that arrival times of surface reflections are delayed with respect to predictions made on the basis of know elastic velocities. This is true both observationally and theoretically based on non-linear finite difference calculations (Trulio et al, 1980; Mellman et al, 1980). In addition, several workers (Bache et al, 1979; Blandford et al, 1979) have presented observational evidence that at least at high frequencies, amplitudes of surface reflections can be greatly reduced compared to estimates based on linear elastic theory. These amplitude effects can be seen, once again, in theoretical non-linear models. We would like any inversion technique to include these effects.

While anomalous amplitude and travel times of surface reflections can, to some extent, be estimated using traditional modeling techniques (Burdick and Helmberger, 1979)

uncertainties in time function and attenuation operators limit the resolution obtainable. In such circumstances, we expect that relative waveform methods will be of maximum utility.

If we restrict ourselves to consideration of events of approximately the same size in the same source region (and thus, presumably in the same geologic material), recorded at the same teleseismic station, it is reasonable to assume that the major differences in seismograms for different events will be caused by an overall scale factor change and changes in pP travel time and amplitude. We therefore choose the common portion of the synthetic seismograms, T(t) in equation 2, to include the normalized source time function, geometric spreading, anelastice attenuation, receiver function and instrument transfer function. The functions $S_i(t)$ are of the form

$$S_1 = c_1 \left(\delta(t) - a_1\ \delta(t-t_1)\right) \tag{5}$$
$$S_2 = c_2 \left(\delta(t-t_o)-a_2\ \delta(t-t_o-t_2)\right).$$

In order to reject the trivial minimum of error functional e_{12} in equation 4, namely $c_1 = c_2 = 0$, we impose the constraint

$$c_1 \cdot c_2 = 1 \quad \text{or equivalently} \tag{6}$$
$$c_1 = 1/c$$
$$c_2 = c.$$

For parametrization of more than two S_i, we procede as above, with the constraint $\Pi c_i = 1$. In this case, we minimize a new error function

$$e^2 = \sum_{i>j} \frac{1}{c_i \, c_j} e_{ij}^2 . \tag{7}$$

For simplicity, however, we will restrict the following discussion to the two event case.

At this point, it is convenient to define a new normalized concatinated function E_n. This is formed by concatinating functions $V_i F^i{}_{12} * W$ where $W'(\omega)=1+k\omega$. The concatinated functions are then sampled at discrete time points . Thus E_n is the nth time point of the concatinated prefiltered and normalized error functions. We note that minimization of

$$\varepsilon^2 \equiv \Sigma (E_n)^2 \tag{8}$$

is equivalent to minimization of the error function e_{12}, but leads to a somewhat more simple formulation.

The actual determination of the S_i is carried out using an iterative stabilized linearized least-squares inverse me thod. We let m_j be the model parameters that define all the s_i. Then some change in model parameters δm_j will cause some change δE_n in the error function E_n. We wish to find δm_j to satisfy $E_i + \delta E_i = 0$ in a least squares sense. By Taylor expansion, we find

$$\delta E_i \cong \frac{\partial E_i}{\partial m_j} \delta m_j \equiv A_{ij} \delta m_j . \tag{9}$$

This gives us the linearized equation

$$A_{ij} \delta m_j + E_i = 0. \tag{10}$$

The weighted least squares solution to this equation is given, in matrix notation, by

$$\delta m = -(A^T A + \gamma I)^{-1} A^T E \tag{11}$$

where $\gamma = \sigma$ trace $(A^T A)$ is a damping factor used to stabilize the inversion. The form of A, the derivative matrix, is given in the appendix. The inversion procedure is applied iteratively, so that the model estimate m_j^{k+1} after k+1 iterations is given by

$$m_j^{k+1} = m_j^{k+1} + \delta m_j^{k+1}. \tag{12}$$

We note that, due to the non-linearity of the problem, the matrix A_{ij} must be recomputed at each iteration.

The form of the error function in equation 3 and the model parametrization used give the relatvie waveform inversion several interesting properties. In general, differences in pP times and amplitudes for two events will be

much better constrained than the amplitude or travel time of and individual pP. As an example, consider the case in which seismograms for two events are identical. Thus

$$f_1(t) = f_2(t) \text{ and}$$
$$s_1 * f_2 - s_2 * f_1 = 0 \quad \text{if } s_1 = s_2. \tag{13}$$

In this case, there are no constraints on individual pP times or amplitudes at all, while time and amplitude differences for the two events remain well-constrained. Resolution of individual times and amplitude improves as two events become increasingly dissimilar. This fact is borne out by examination of the model varience matricies for synthetic and actual data runs.

Another interesting aspect of relative waveform inversion is the ability to determine pP arrival times even when these times are less than the inverse of the high frequency cutoff for bandpassed data. This is due to the fact that the norm of the error function, viewed in the frequency domain, is minimized by matching phase at all available frequencies. This is in contrast to cepstal methods, for instance, which require that two arrivals have a π phase shift at some frequency in order to produce an arrival time estimate.

If this frequency is high enough to be outside usable signal passband, or if the second arrival is not a spectral shadow of the first arrival at high frequencies, the cepstral method will fail. Under these circumstances, the

relative waveform inversion will still produce a reliable estimate valid in the data passband.

Although much of the development in this section has been done in terms of a specific problem, the basic relative waveform method has far more general applicability. The error function defined in equation 3 and its rather straightforward generalization to multiple receivers and many events, is in no way tied to the specific source estimation problem in question. In particular, one example in which the relative waveform method is likely to yield good results is in the estimation of earth structure controlling triplications. Conventional modeling methods are quite powerful in this type of problem, but suffer from the necessity of obtaining good source and attenuation estimates, even though both source and attenuation are stationary over the distance range of interest. Thus, such studies often must be preceded by detailed source studies, while use of short period waveform data is precluded due to the lack of adequate source models at short periods. By using the relative waveform method for all possible pairs of observations for a given event, and including a number of events, move out and relative amplitude information may be recovered from waveforms without the necessity of detailed source studies.

As in any other method, the validity of the results of a relative waveform inversion depends on the validity of the assumptions that go into the method. We would therefore

like to delineate the assumptions made, and to explore the effects of these assumptions, where possible.

For tightly grouped events observed at a single station, it is reasonable to assume that attenuation, instrument transfer function, and receiver function will be common for all events. Use of a single source time function for all events, however, is less easily justified. It is certainly unjustified for events of greatly different size or events occuring in grossly different materials, such as granite and unsaturated sediments. If, however, the events are in similar materials, it is anticipated that the degree of overshoot in the time functions of the two events will be similar (Haskell 1967). Also, for small to intermediate events, changes in the rise time of the source time function will produce only minor effects in the final seismogram. This has, to some degree, been tested using synthetic source functions derived from finite difference calculations by Perl and Trulio, 1981, for a variety of events. Results of synthetic studies on source function bias in relative waveform inversions using von Seggern-Blanford sources are presented in a later section.

A second cause for concern lies in the use of a single, frequency independent arrival to represent all of the nonconstant effects of near source propogation. Certainly, in the presence of complex crustal structure, small changes in source location can result in differing numbers, amplitudes and arrival times for crustal reflections. Also, as men-

tioned earlier, evidence exists for the frequency dependence of the amplitude of the surface reflection.

Both time function and propagation effects can easily be explicitly included in the inversion model. Unfortunately, the limited bandwidth available in observed seismograms makes it doubtful that any of these effects could be differentiated from a simple change in pP amplitude or arrival time. For this reason, it was decided to allow all variation to occur in the surface reflection, and to investigate resolvability of additional early arrivals at a later date.

How, then, are we to interpret the results of a relative waveform inversion? Clearly the second arrival in a narrow frequency band a time corresponding to some weighted average of these arrival times. To the extent that these arrivals are dominated by pP, the second arrival time and amplitude will be accurate estimates of pP delay and average amplitude within a narrow spectral window. The estimated overall amplitude factor, however, can be expected to remain valid independent of the exact nature of the constituents of the second arrival. Alternatively, if the results of the relative waveform inversion may be viewed as providing a measure of the degree of difference of observed seismograms, expressed in terms of a simple, plausible source model. At the very least, this provides a mechanism for identifying events that are anomalous, or at least show large differences from other events in ways that cannot be explained

by very small changes in pP time and amplitude. And again, the important fact in adjusting yield estimates is the size and timing of the effective second arrival, not the physical causes of this arrival.

An additional assumption of source isotropy is made when data from several stations at widely differing azimuths is used in the same inversion run. In cases of large scale tectonic release, asymmetric spall, or lateral variation in structure, the effective source function s_i for a given event may show significant azimuthal variation. A comparison of errors for an inversion containing data sampling a range of azimuths with inversions contain data sampling single azimuths should provide a means of assessing, and studying, azimuthal source variations.

III. SYNTHETIC RESULTS

A series of tests on synthetic data were conducted to test the relative waveform inversion methodology and its sensitivity to variations in input parameters, in data and source characteristics, and in inversion parameters. Some results of the first set of test cases are illustrated in Figures 1 and 2. These experiments examined the sensitivity of the technique to choice of starting values (with respect to the true values) and to selection of the damping parameter in the actual inverse procedure. Two synthetic short period P wave seismograms were constructed for these tests. Both seismograms have identical instrument, attenuation, and source time function characteristics, differing only in the time delay and amplitude of the second (pP) arrival (see Figure 1). In order to examine the effect the choice of starting model, the inverse assumed initially that both seismograms had the same pP delays and amplitudes and iterated from that point. In addition, this procedure was repeated using a different value of the damping parameter σ. The results of both tests are shown in Figure 2. We see that in both of these particular examples, fairly rapid convergence to the correct values was attained. Figure 3 compares the derived waveforms following the inverse procedure. The rate of convergence is, of course, controlled by the inversion damping parameter. Although in the present example both σ values (0.01 and 0.001) permitted stable convergence, further testing has shown that the choice of 0.01

SYNTHETIC SEISMOGRAMS

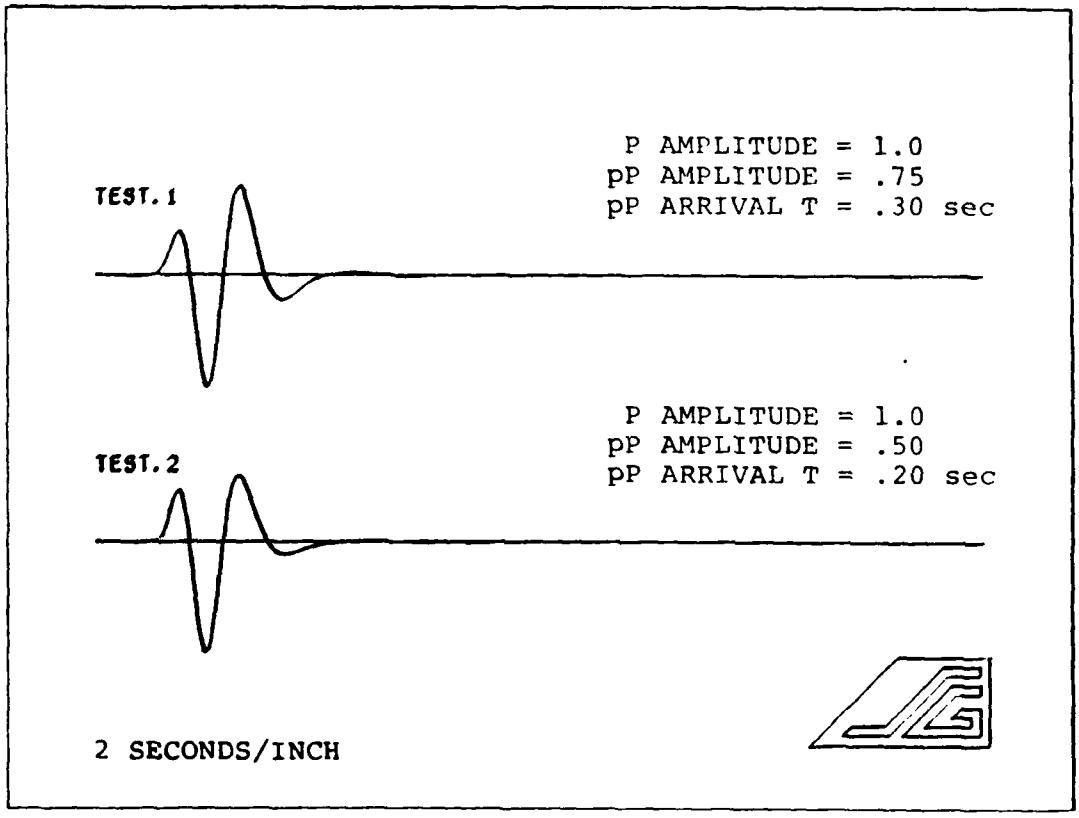

Figure 1. Two test synthetics were constructed to check the convergence of relative waveform inversion. The synthetics have the same instrument response, attenuation and time function convolved together with different pP spike arrivals. T#1 has a pP spike arrival at .30 sec. with an amplitude of .75 (Rel. to P) while T#2 has a pP arrival at .20 sec. with an amplitude of .50.

Figure 2. Using our two synthetic seismograms we invert for pP arrival time and amplitude given a starting estimate. In this graph of pP amplitude versus arrival time we have selected our starting position at .6 and .4 sec. The inversion successfully converged from this point to correct synthetic amplitudes and arrival times. We ran the inversion with two different damping factors to illustrate convergence stability.

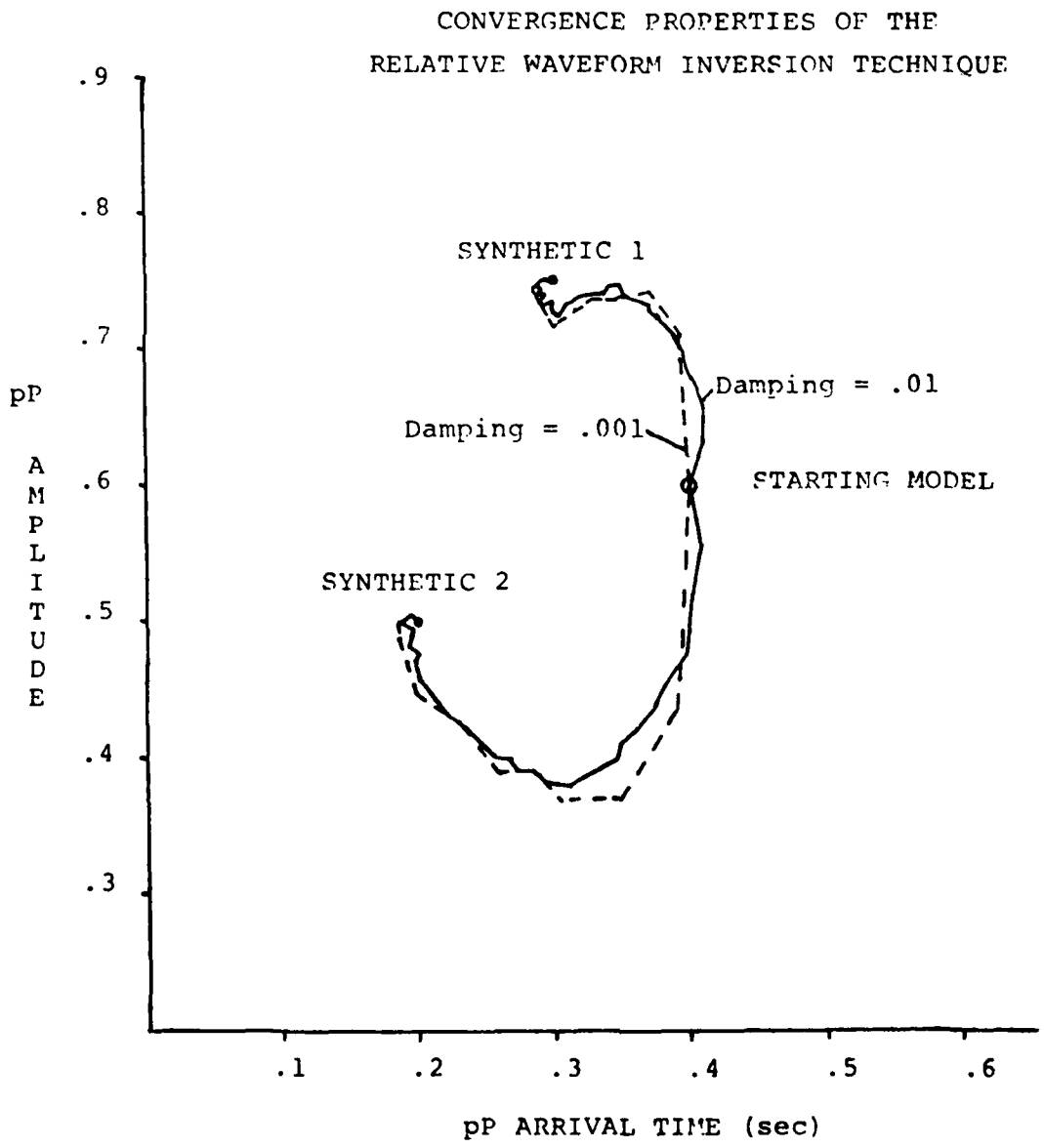
CONVERGENCE PROPERTIES OF THE
RELATIVE WAVEFORM INVERSION TECHNIQUE
.9
.8
.7
.6
.5
.4
.3
pP
AMPLITUDE
SYNTHETIC 1
Damping = .01
Damping = .001
STARTING MODEL
SYNTHETIC 2
.1
.2
.3
.4
.5
.6
pP ARRIVAL TIME (sec)

Figure 2:

Figure 3:

In this figure we have the inversion results from our test synthetics. We have inverted for two spike seismograms S1 and S2 which converged to the source terms convolved into our synthetics. Given one synthetic then, F1 we can construct a duplicate of F1 by convolving the transfer function (S1/S2) with F2. F1 and F2* (S1/S2) are shown here for comparison. If the inversion has converged to the exact solution, which it has in this case, then these two seismograms will be identical.

PARAMETERS

A1=	0.7569	TAU=	-0.0004
A2=	0.5050	TAU1=	0.2860
C=	1.0010	TAU2=	0.1933

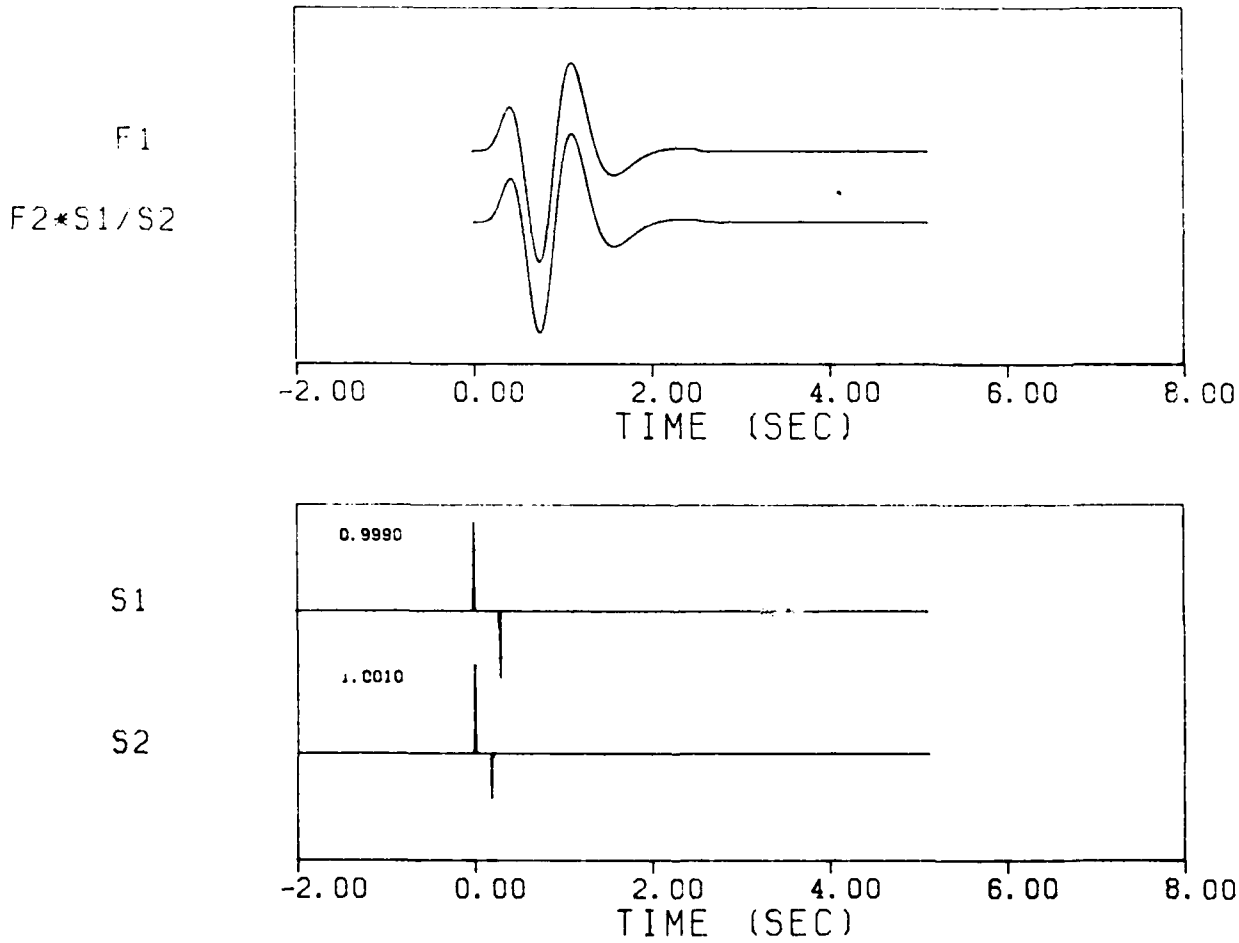

Figure 3:

is highly preferred. While this value results in somewhat slower convergence, it is always a stable procedure. While the smaller damping afforded by a $\sigma = 0.001$, causes generally faster convergence, frequently the smaller damping causes either divergent solutions or a "hem-stitching" behavior in the iterative procedure.

The second series of tests with synthetic data examined the effects of random noise in the data as well as testing for distortion of the final results by such factors as complex receiver functions. Figures 4 and 5 show the basic synthetic data employed, the same data with 10% instrument bandpassed noise added, and the synthetic data convolved with observed receiver functions for the SRO stations CHTO and ANMO. The choice of instrument bandpassed noise was felt to be a most severe test due to the fact that this noise has a similar frequency content to the signals. The convergence path results of two test inversions, utilizing different starting models, of the synthetic data with noise added are shown in Figure 6. Both inversions converged to the same final values which differ slightly from the true parameters. However, these noise-induced errors were generally very small (less than 10% in pP amplitude and less than 0.1 second in pP delay time).

Since the near-receiver crustal response is a common feature in the data, theoretically it should have no influence upon a relative waveform inversion. However, to test this basic assumption, especially in light of the

Figure 4. Shown above are four basic synthetic seismograms used to simulate one of the two station seismograms needed for relative waveform inversion. The first synthetic has only an instrument, source time function, attenuation operator and spike (P,pP) seismogram convolved together. In addition the second trace has 10% random instrument filtered noise added to it. Synthetics 3 and 4 have know receiver functions for SRO stations CHTO and ANMO convolved in instead of noise.

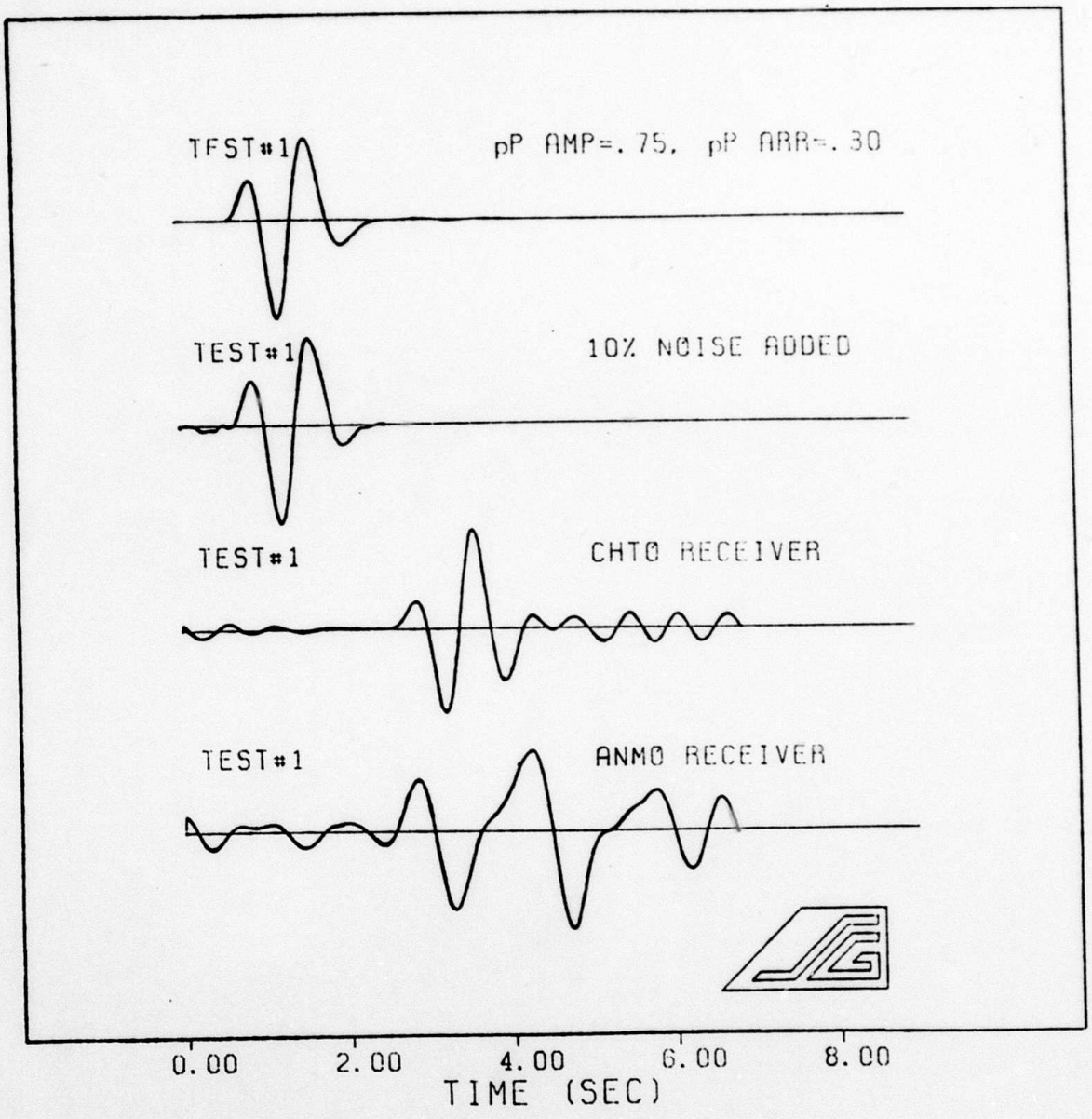
TEST#1
pP AMP=.75, pP ARR=.30
TEST#1
10% NOISE ADDED
TEST#1
CHTO RECEIVER
TEST#1
ANMO RECEIVER
0.00
2.00
4.00
6.00
8.00
TIME (SEC)

Figure 4:

Figure 5. Shown above are four basic synthetic seismograms used to simulate one of the two station seismograms needed for relative waveform inversion. The first synthetic is composed of an instrument, source time function, attenuation operator, and spike (P,pP) seismogram. In addition to these convolution terms, the second trace has 10% random instrument filtered noise added to it. Synthetics 3 and 4 have known receiver functions for SRO stations CHTO and ANMO convolved in instead of noise.

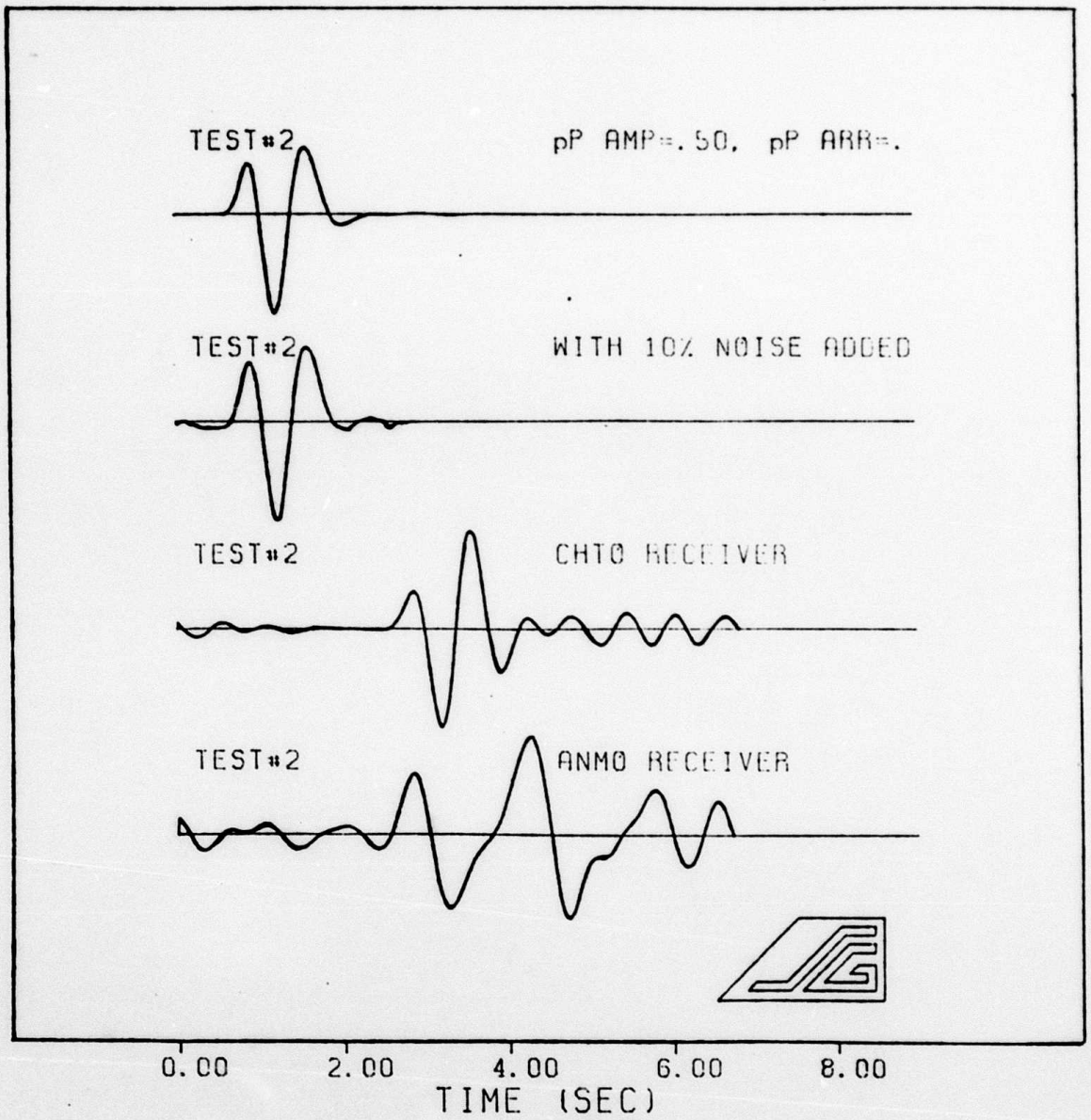
TEST#2
pP AMP=.50, pP ARR=.
TEST#2
WITH 10% NOISE ADDED
TEST#2
CHTO RECEIVER
TEST#2
ANMO RECEIVER
0.00
2.00
4.00
6.00
8.00
TIME (SEC)

Figure 5:

Figure 6:

Relative waveform inversion was performed on the two test synthetics with random 10% instrument bandpassed noise added to each signal. Using the same two starting models we plotted the inversion path in term of P^P amplitude versus arrival time. The maximum error in this test was only 10% in amplitude and 0.1 seconds which may be reduced (by $\sqrt{N}$) by adding more stations to the inversion.

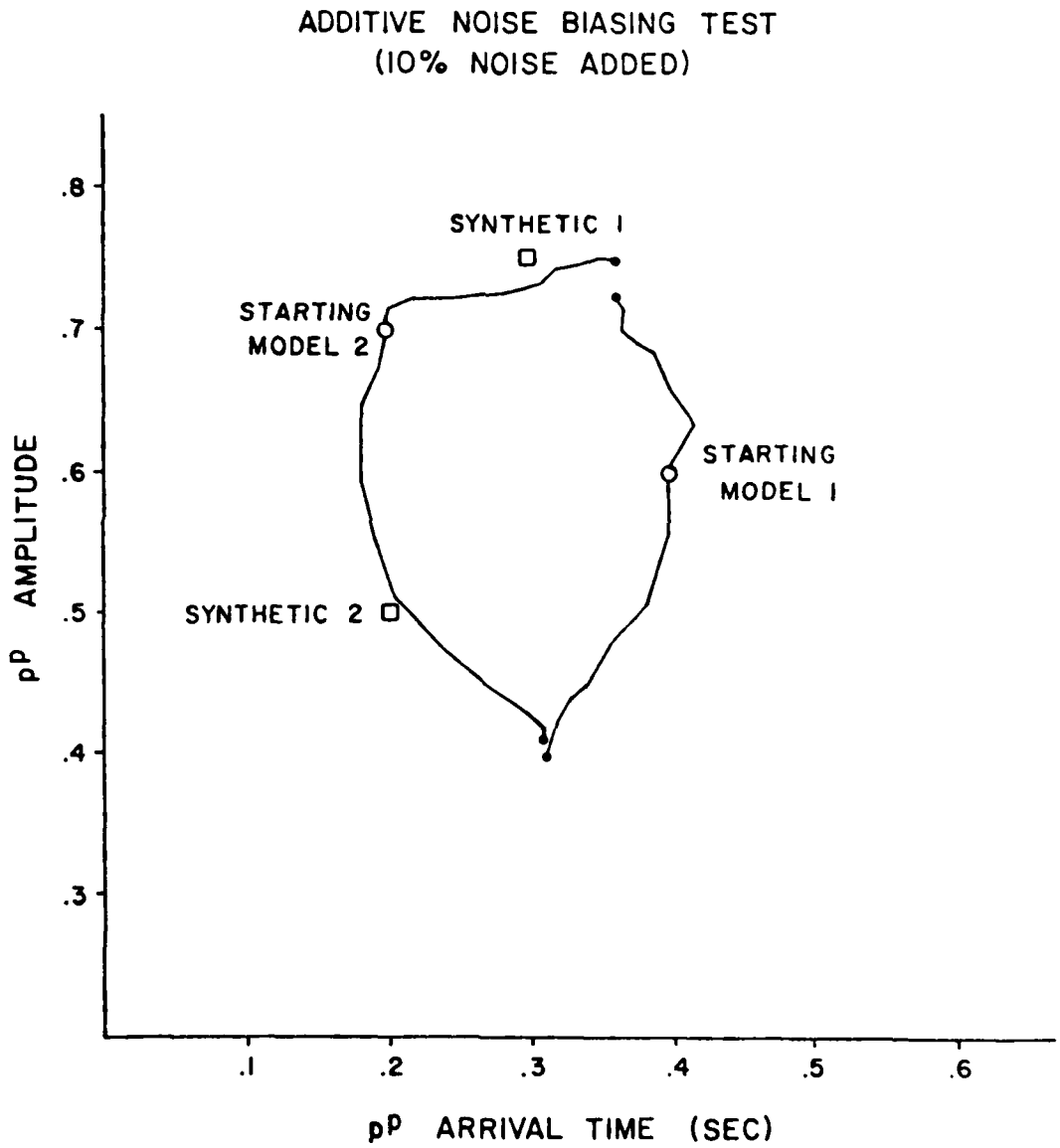
ADDITIVE NOISE BIASING TEST
(10% NOISE ADDED)
SYNTHETIC 1
STARTING MODEL 2
STARTING MODEL 1
SYNTHETIC 2
pP AMPLITUDE
.8
.7
.6
.5
.4
.3
.1
.2
.3
.4
.5
.6
pP ARRIVAL TIME (SEC)

Figure 6:

occasionally very complex nature of the near-receiver effects, the influences of the receiver effects at the SRO stations CHTO and ANMO (Figures 4 and 5) were specifically tested. Since both of these stations were used extensively in the applications of this technique to observed data, this was felt to represent a particularly important test. Figures 7 and 8 plot the convergence paths for the inversion test using the ANMO and CHTO receiver functions. A maximum error of 6% was observed.

In all of the tests conducted, the errors introduced by outside factors were encouragingly small in relative P wave amplitude, pP amplitude, and pP delay time. Moreover, even these relatively small errors can be further reduced by utilizing more than two stations in the inversion procedure.

The final series of synthetic data tests examined the influences of source time function on the technique. The assumption that the source time function is identical amoung the events examined would seem to be the most questionable, and these part of the study attempts to quantify the effective bias, if any, introduced by variations in source time function. Synthetic data were constructed using von Seggern and Blandford (1972) source functions with a distribution of overshoot and rise time characteristics. The von Seggern - Blandford source time function, in the far-field, is given by:

Figure 7. The observed receiver function for SRO station ANMO was convolved with both our test synthetics before inversion. Shown here are the convergence paths from two different starting models plotted in pP amplitude-arrival time space. Station ANMO has a slightly greater effect on convergence than did CHTO no doubt because it acted as a lowpass filter and eliminated necessary high frequency waveform details.

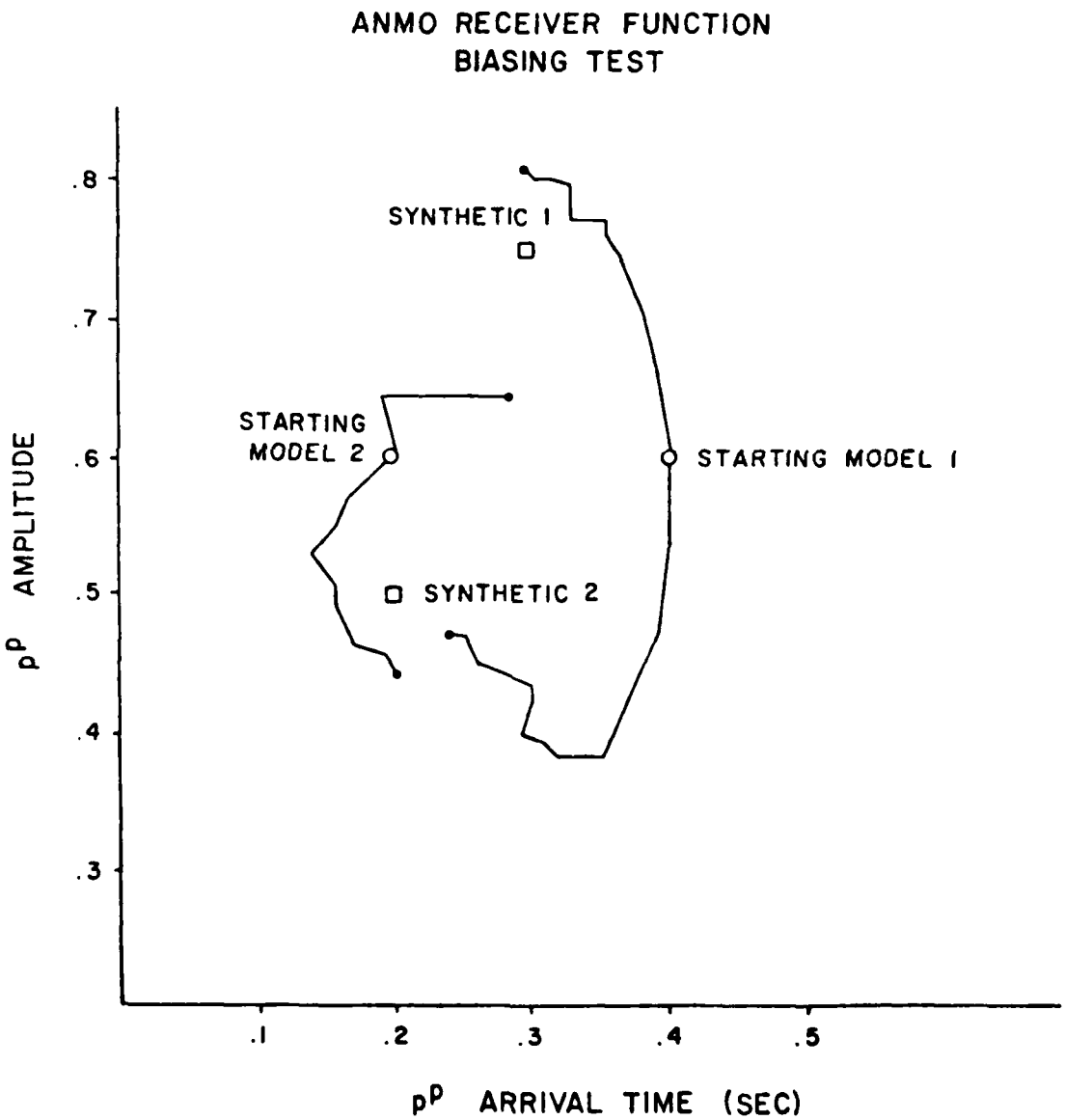
ANMO RECEIVER FUNCTION
BIASING TEST
SYNTHETIC 1
STARTING MODEL 2
STARTING MODEL 1
SYNTHETIC 2
.8
.7
.6
.5
.4
.3
pP AMPLITUDE
.1
.2
.3
.4
.5
pP ARRIVAL TIME (SEC)

Figure 7:

Figure 8. A receiver function for the SRO station CHTO was convolved with our two test synthetics before inversion to check common filtering effects. Shown above are the inversion paths from two different starting models plotted in terms of pP amplitude versus arrival time. As expected the common convolution factor has very little effect on convergence.

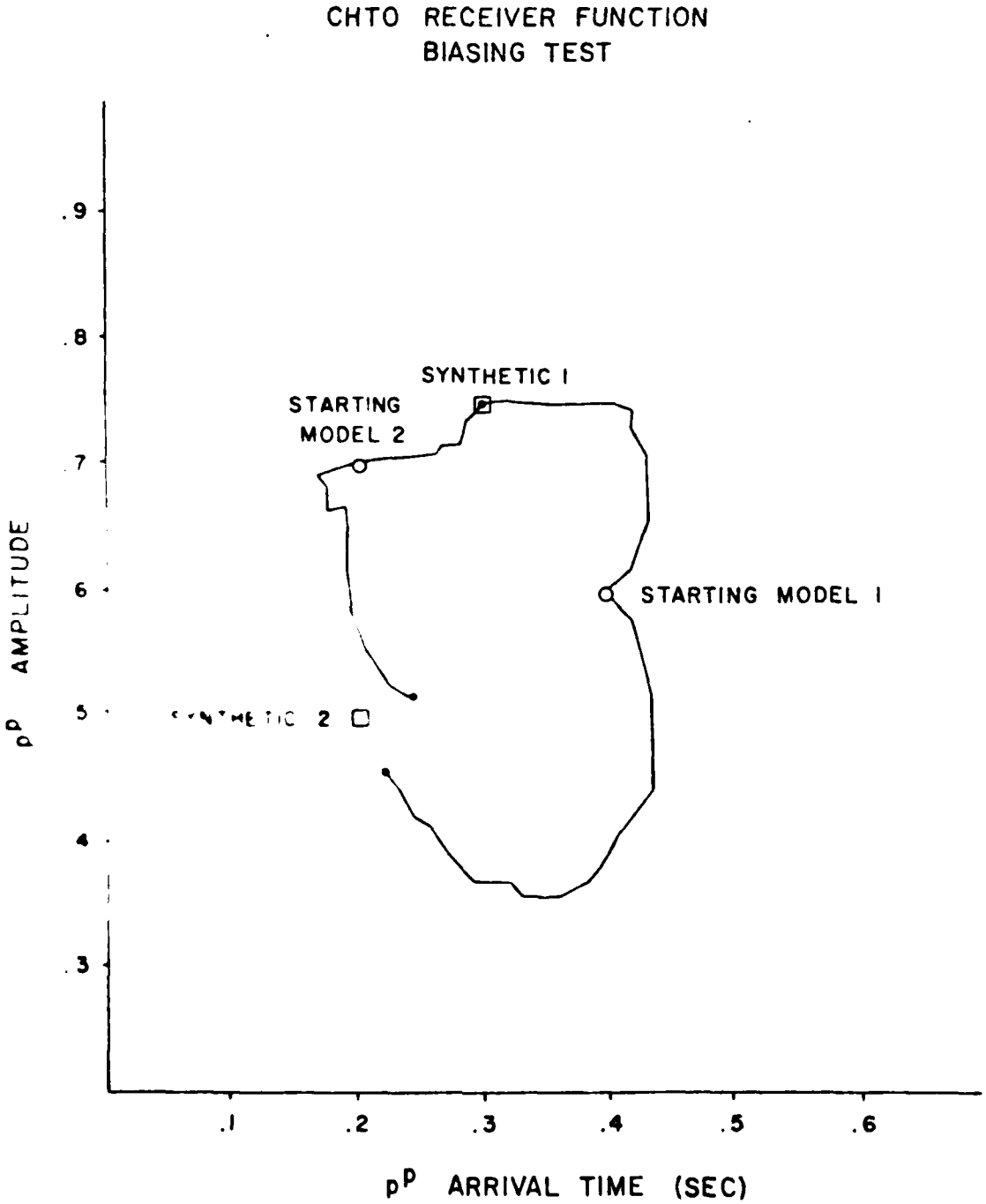
CHTO RECEIVER FUNCTION
BIASING TEST
SYNTHETIC I
STARTING
MODEL 2
STARTING MODEL I
SYNTHETIC 2
.9
.8
.7
.6
.5
.4
.3
.1
.2
.3
.4
.5
.6
pP AMPLITUDE
pP ARRIVAL TIME (SEC)

Figure 8:

$$V(\tau) = \gamma_o \, ke^{-k\tau} \left((1+2B)k\tau - Bk^2 \tau^2 \right)$$

where k is the risetime parameter, B controls the degree of overshoot, and γ_o is an overall sealing factor. We shall be only concerned here with examining the effects of variations in k and B.

Typical values of k and B for an event with a yield on the order of 100 kt are 10 and 1 respectively. For the purposes of these inversion tests, these values were selected as the mean and variations about these values were used to construct the test dataset. Graphical representations of the source time functions with k varied between 5 and 15 and B varied between 0 and 3 are shown in Figure 9. The synthetic siesmograms were constructed by convolving the time functions shown in Figure 9 with a short period SRO instrument response, an attenuation operator, δ-function P and pP arrivals and CHTO and ANMO receiver functions. The final synthetics are shown in Figures 10 and 11. In all cases, the pP arrival was inserted with a .4 second time delay and an amplitude of .8 relative to the direct P wave.

A series of two station inversion tests were conducted using the standard (k=10, B=1) synthetic seismogram and the other synthetic data. The starting point in each test was the true values (pP amplitude = .8; pP delay = .4 sec.). One important factor noted here and in all previous tests was that the inversion becomes more constrained and resolution increases apparent differences in the observed waveforms increase.

Figure 9a:

Source time functions from the Von Seggern and Blandford model are shown above for a range of risetimes with fixed overshoot (B=1). From these time functions we construct station synthetics and test for inversion bias due to a variable source term.

Figure 9b:

Source time functions shown above cover a range of overshoot with the risetime fixed at K=10.

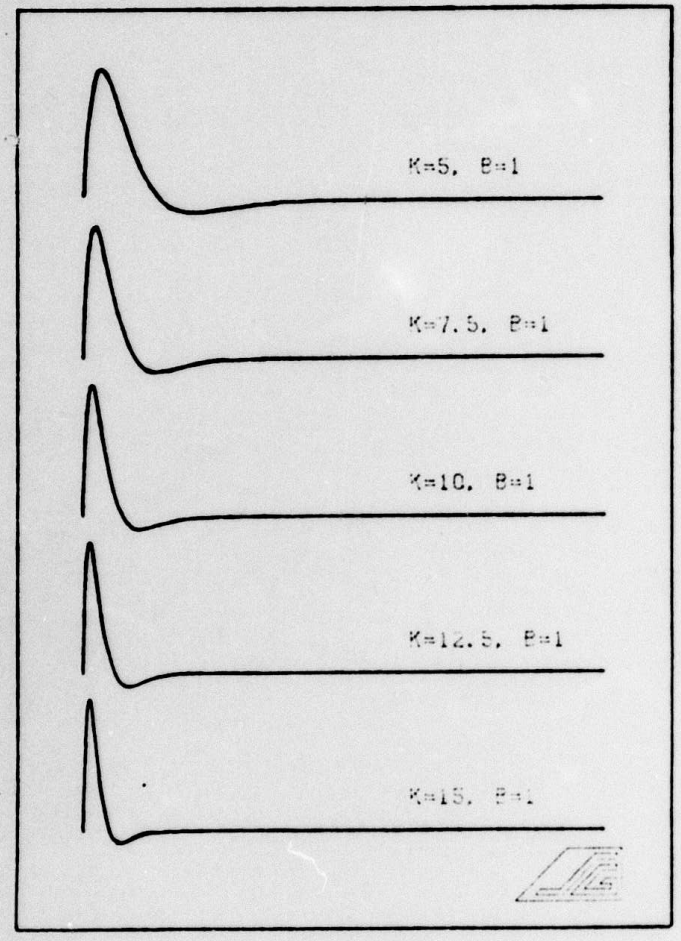

Figure 9a:

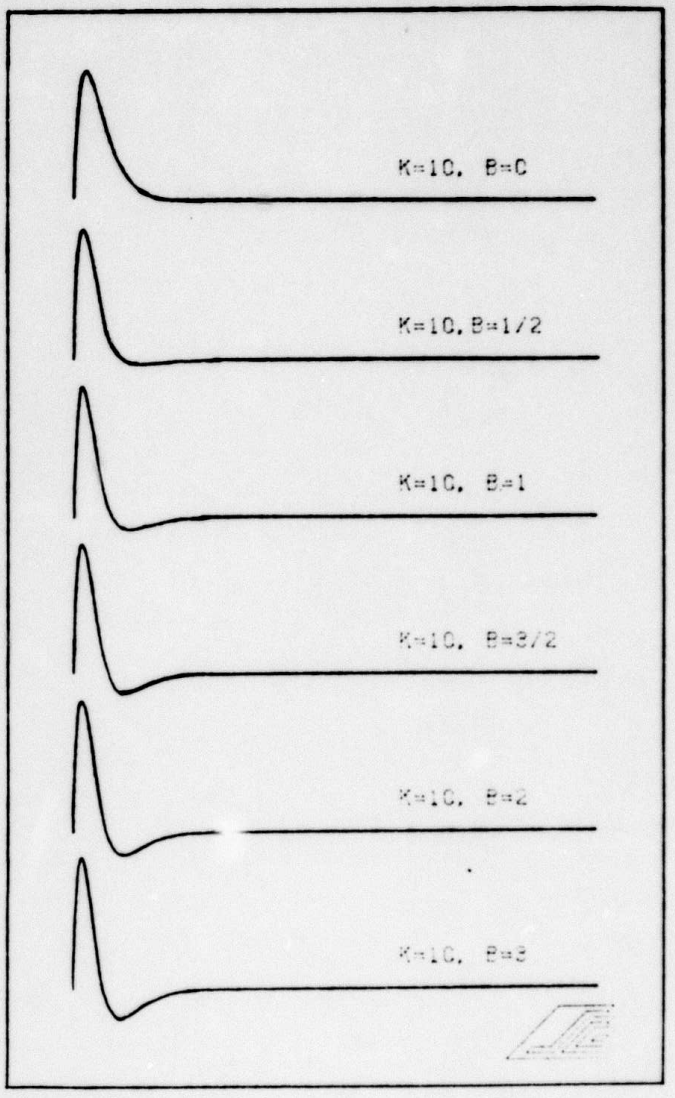

Figure 9b:

Figure 10a:

Synthetic seismograms are shown for a range of overshoot parameter B and constant rise time K. Receiver function appropriate for CHTO has been used.

Figure 10b:

As in Figure 10a, but with ANMO receiver function.

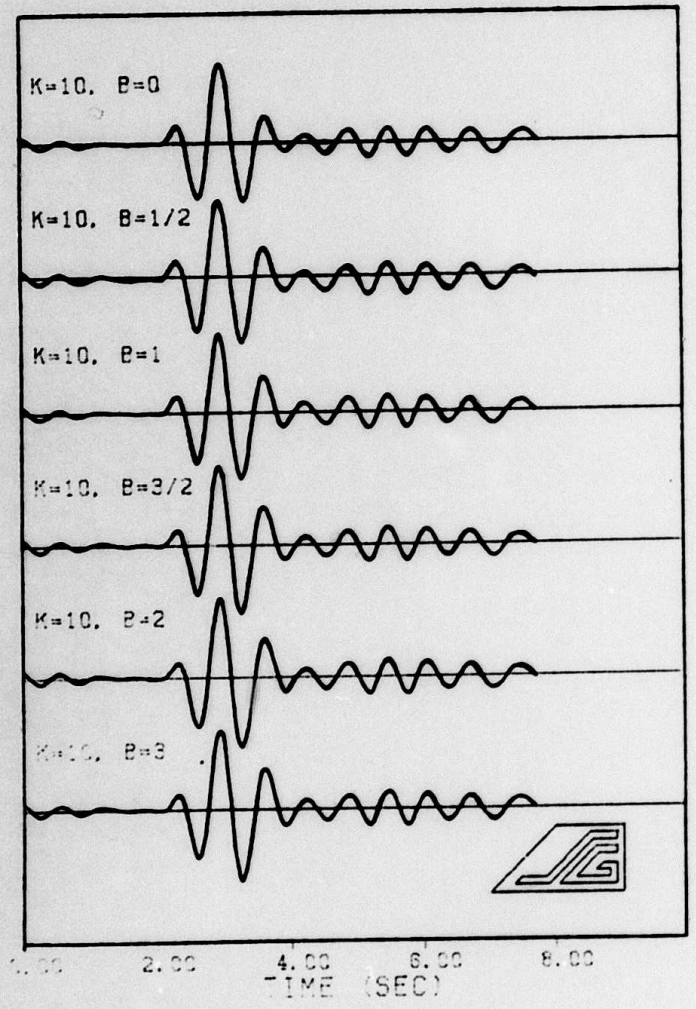

Figure 10a:

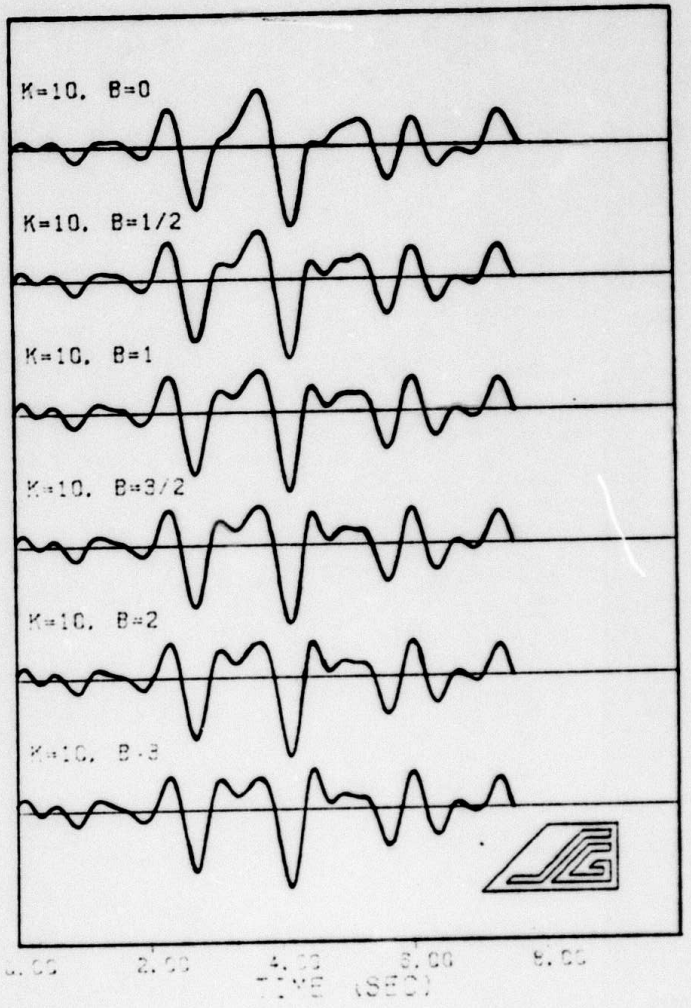

Figure 10b:

Figure 11a. Synthetic siesmograms are shown for a range of risetime parameters K with constant overshoot B. Receiver function for CHTO has been used.

Figure 11b. As in figure 11a buth with ANMO receiver function.

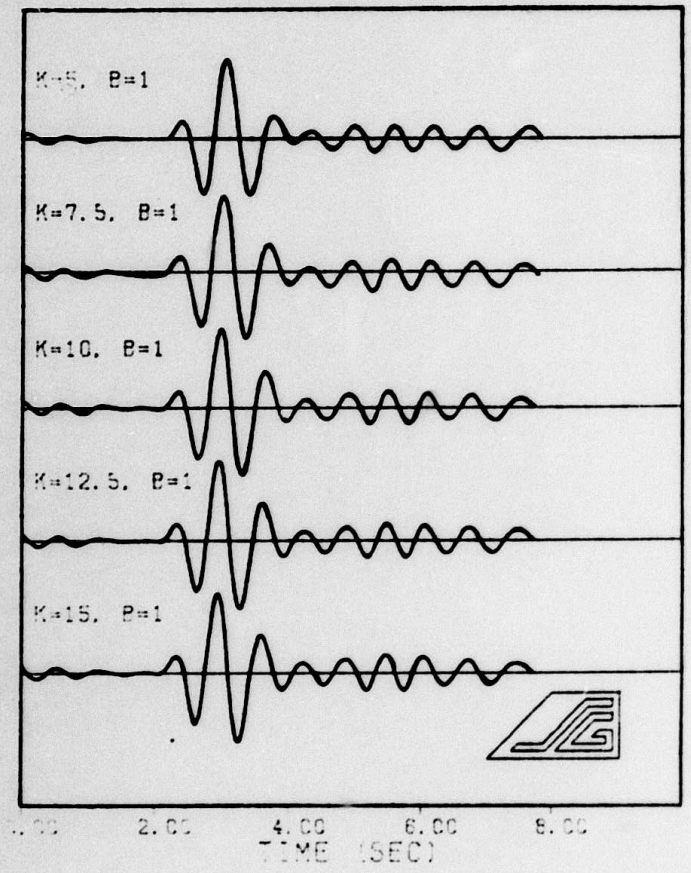

Figure 11a:

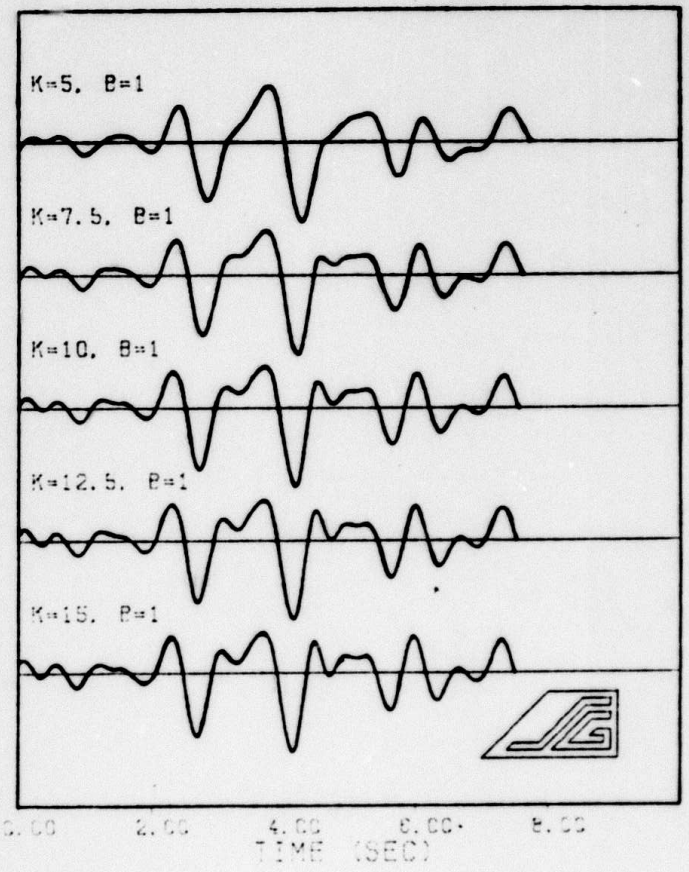

Figure 11b:

We first consider the effects of variations in overshoot parameter. Figure 12 illustrates the biasing effect of changes in overshoot on the results of the relative waveform inversion. In general, the derived pP arrival time (Figure 12b) is little effected by changes in overshoot. Only in the extreme case of a 0:1 ratio in the B value between the two seismograms does the error exceed .02 seconds and even then the error reaches only 0.07 seconds. The derived pP amplitude is somewhat more sensitive (Figure 12a) although again the bias exceeds about 15% only when the ratio of B values becomes extreme (0:1 or 3:1). In practice, such changes are unlikely to be encountered in the observed data sets we contemplate.

Figure 13 summarizes the effects of variations in risetime (k) on the method. Here we find somewhat of a reversal in trend in comparison to the time and amplitude variations produced by changes in the B value. The pP amplitude is almost insensitive to variations in k except at the extremal 5:10 ratio where the error approaches as much as 25%. Delay time is more sensitive to k variations than to changes in B but again errors exceed 0.03 seconds only at a 5:10 ratio and only reach .06 at that extreme. The larger k values have much reduced biasing effect because of the filtering effects of the instrument response.

In total, the effect of assuming the same source time function seems to not produce significant bias to our estimates of pP amplitudes and delays. In light of those

Figure 12. Inversion solutions for synthetic problem investigating the effect of changes in rise time parameter K for Von Seggern-Blanford source. Reference event has K=10, B=1 but K varying from 5 to 15. Only for extreme model (K=5) does significant bias occur.

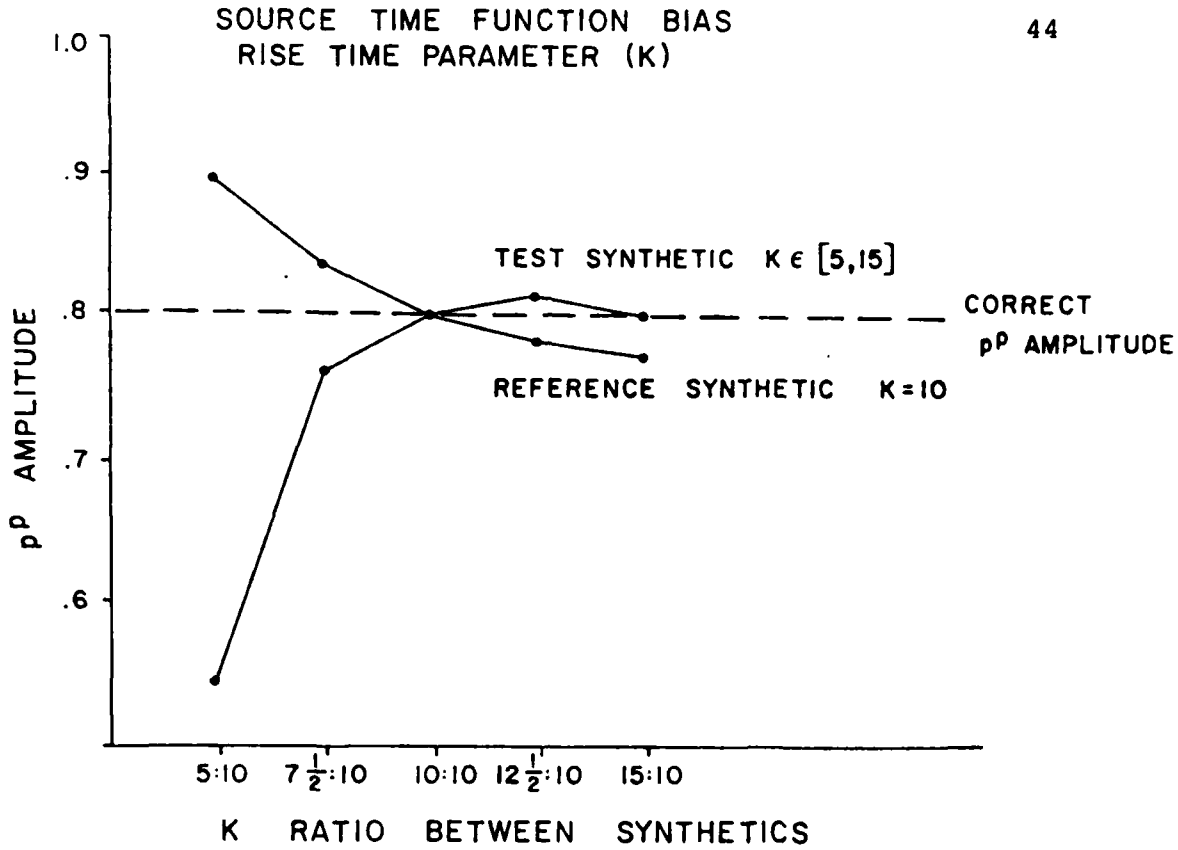
SOURCE TIME FUNCTION BIAS
RISE TIME PARAMETER (K)
1.0
.9
.8
.7
.6
pP AMPLITUDE
TEST SYNTHETIC K ∈ [5,15]
CORRECT
pP AMPLITUDE
REFERENCE SYNTHETIC K=10
5:10
7½:10
10:10
12½:10
15:10
K RATIO BETWEEN SYNTHETICS

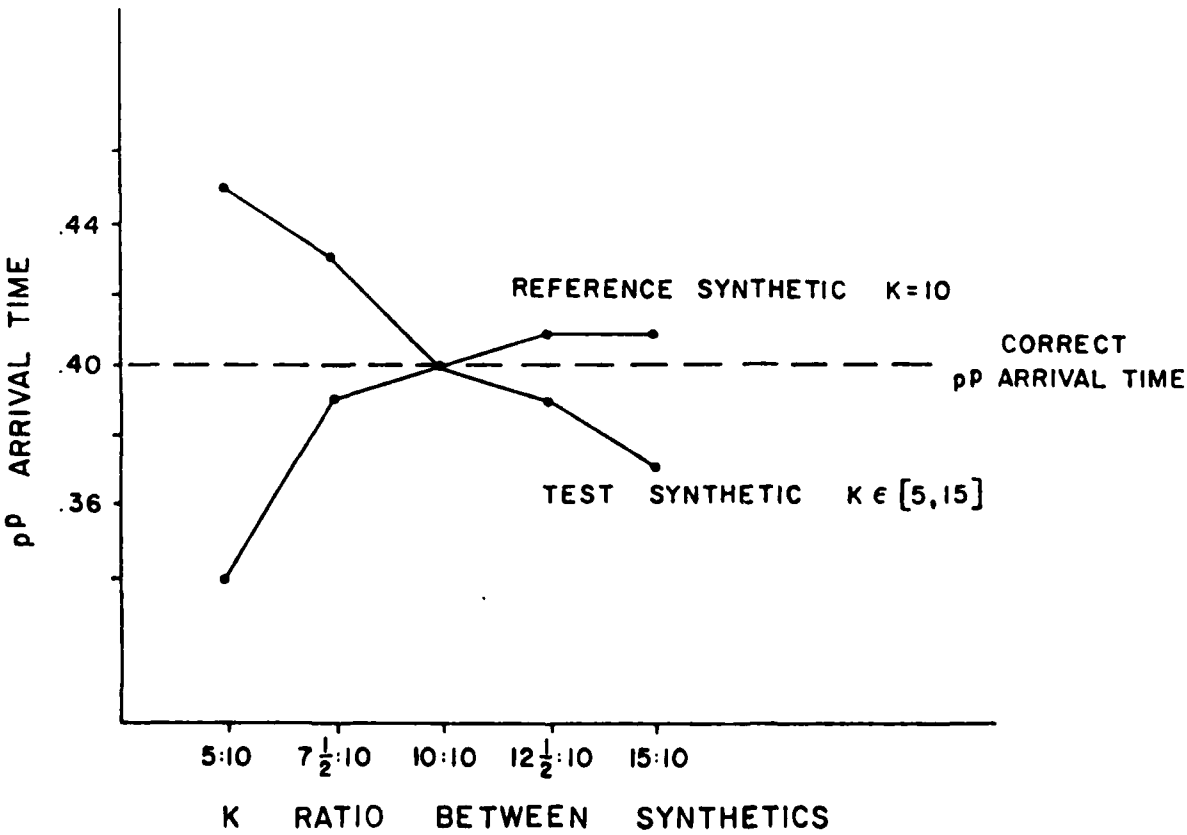
.44
.40
.36
pP ARRIVAL TIME
REFERENCE SYNTHETIC K=10
CORRECT
pP ARRIVAL TIME
TEST SYNTHETIC K ∈ [5,15]
5:10
7½:10
10:10
12½:10
15:10
K RATIO BETWEEN SYNTHETICS

Figure 12:

Figure 13:

Inversion solutions for synthetic problem investigating the effects of changes in overshoot parameter B for Von Seggern-Blandford source. Reference event has K=10, B=1. Other event has K=10 but B varying from 0 to 3.

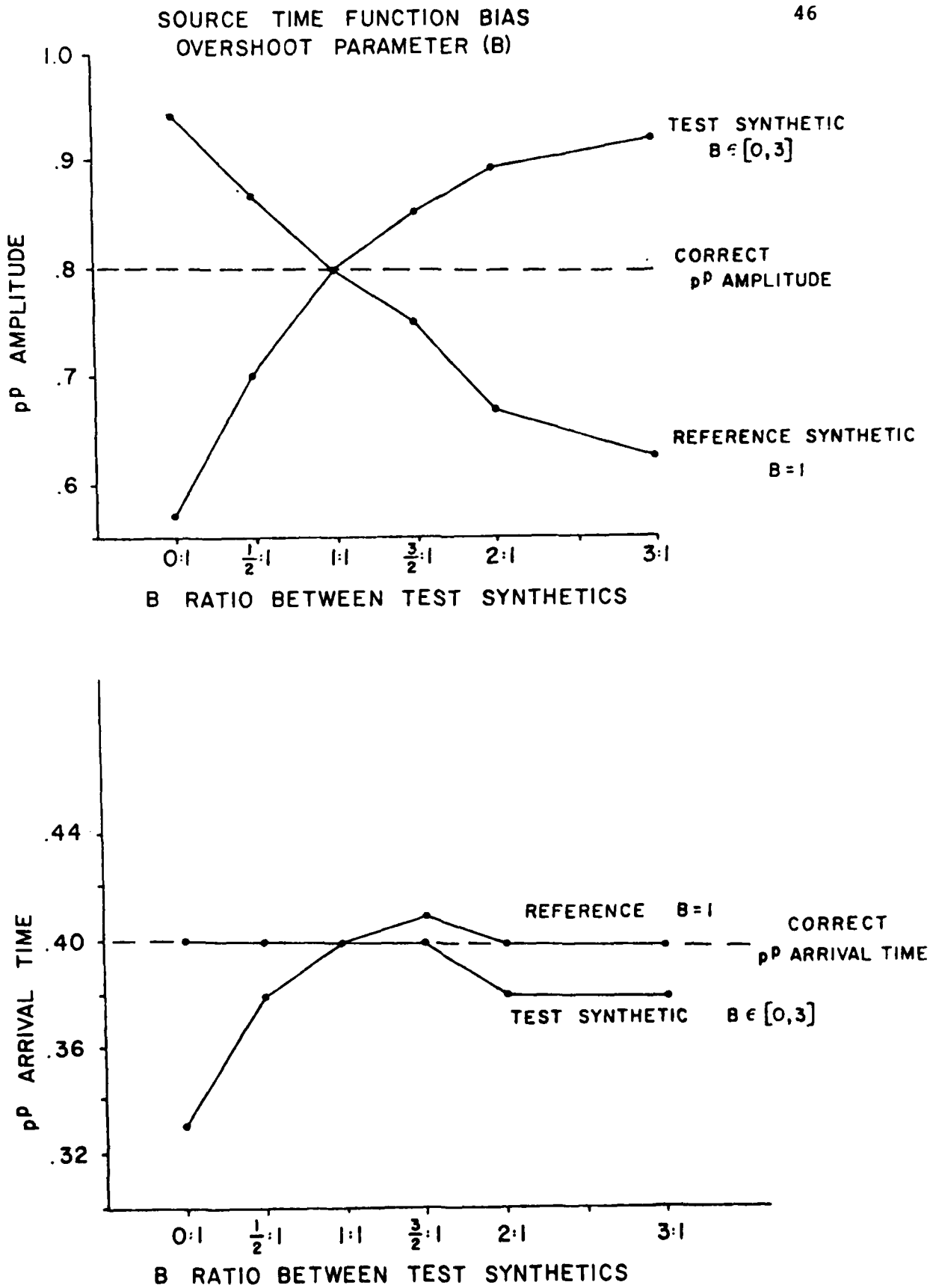
SOURCE TIME FUNCTION BIAS
OVERSHOOT PARAMETER (B)
1.0
.9
.8
.7
.6
pP AMPLITUDE
TEST SYNTHETIC
B ∈ [0,3]
CORRECT
pP AMPLITUDE
REFERENCE SYNTHETIC
B = 1
0:1
1/2:1
1:1
3/2:1
2:1
3:1
B RATIO BETWEEN TEST SYNTHETICS
.44
.40
.36
.32
pP ARRIVAL TIME
REFERENCE B = 1
CORRECT
pP ARRIVAL TIME
TEST SYNTHETIC B ∈ [0,3]
0:1
1/2:1
1:1
3/2:1
2:1
3:1
B RATIO BETWEEN TEST SYNTHETICS

Figure 13:

findings, and of the results of the other parameter studies discussed earlier, we can approach the application of the technique to observed data with confidence. The results of the application of the method to CHTO and ANMO recordings of several Eastern Kazakh events are discussed in the following section.

IV. APPLICATION TO DATA

A suite of seven presumed underground nuclear explosions in Eastern Kazakh, recorded at SRO stations in Thailand (CHTO) and New Mexico (ANMO), were chosen as the data base for the initial application of the relative waveform technique. Good quality digital recordings for all seven were events available at both observatories. In addition, the choice of these two stations provides a range in distance (∿35° to CHTO, ∿95° to ANMO), in azimuth (southeast to CHTO, north to ANMO) from the source region, and in receiver function.

The seismograms at the two stations for all seven events are shown in Figure$ 14 ~~and 15~~, with all traces normalized to unit maximum amplitude. These figures illustrate the fact that the effects in short period seismograms of differing attenuation and near receiver earth structure at two stations can be considerably larger than the effects of differing source time functions and burial depths for two events recorded at a single station. The ANMO seismograms clearly show greater complexity than do the CHTO seismograms, a result of a more complicated receiver function. In addition, the ANMO seismograms clearly show greater attenuation than do the CHTO seismograms.

The seven seismograms recorded at CHTO show relatively subtle differences. These differences are primarily the ratio of first trough to second peak amplitude, width of the

Figure 14:

Data seismograms for all events used in this study at stations CHTO and ANMO. All traces scaled to unit maximum amplitude.

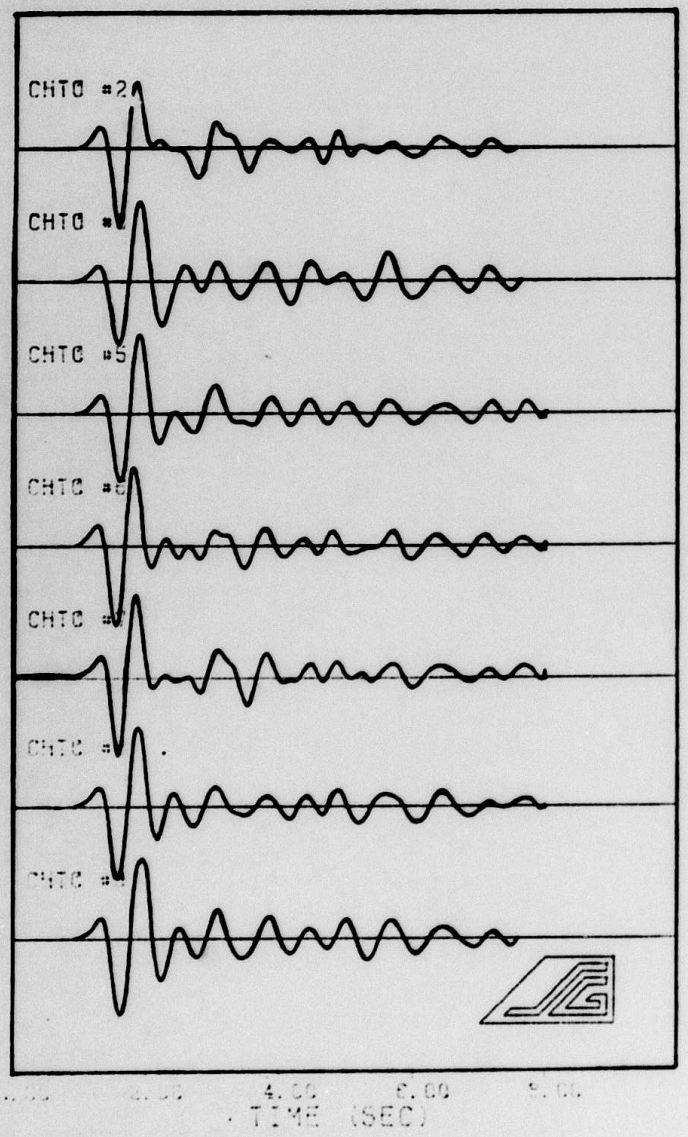
CHTC #2
CHTC #5
4.00
6.00
TIME (SEC)

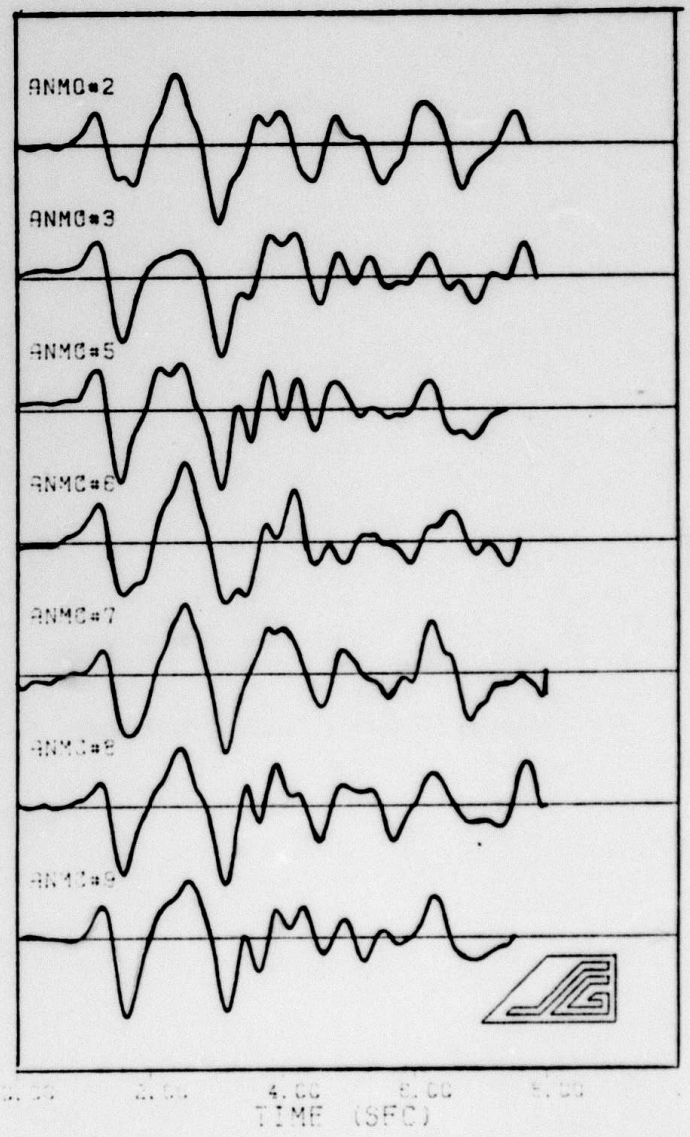
ANMC#2
ANMC#3
ANMC#5
ANMC#7
4.00
6.00
TIME (SEC)

Figure 14:

second peak, and amplitude of the second trough. These differences are consistent in that small second trough amplitude correlates with a narrow second peak. This is the type of effect we expect to see if the waveform differences are caused by changes in pP time and amplitude. It is also worthy of note, at this point, that two pairs of seismograms at CHTO show striking similarity. Events 5 and 8 have virtually identical seismograms, as do events 6 and 7. These event pairs are shown in Figures 15 and 16.

The greater complication of the ANMO receiver function unfortunately prevents identification of simple, correlated differences between events as was apparent at CHTO. Further, it is of some interest to note that greater differences exist for event pairs 5 and 8, and 6 and 7, at ANMO than were apparent at CHTO.

One method of applying the relative waveform inversion technique is a simultaneous inversion of all seven events. An alternative method is to use a weighted regression technique on the results of two and three event inversions, with the weightings determined by the model variance matricies obtained for each inversion run. The latter method was used in this study.

In evaluating the behavior of the relative waveform inversion technique, it was found that the absolute pP amplitudes and delay times were generally less well-constrained than the differences in amplitudes and delay times between different events. This suggests that more

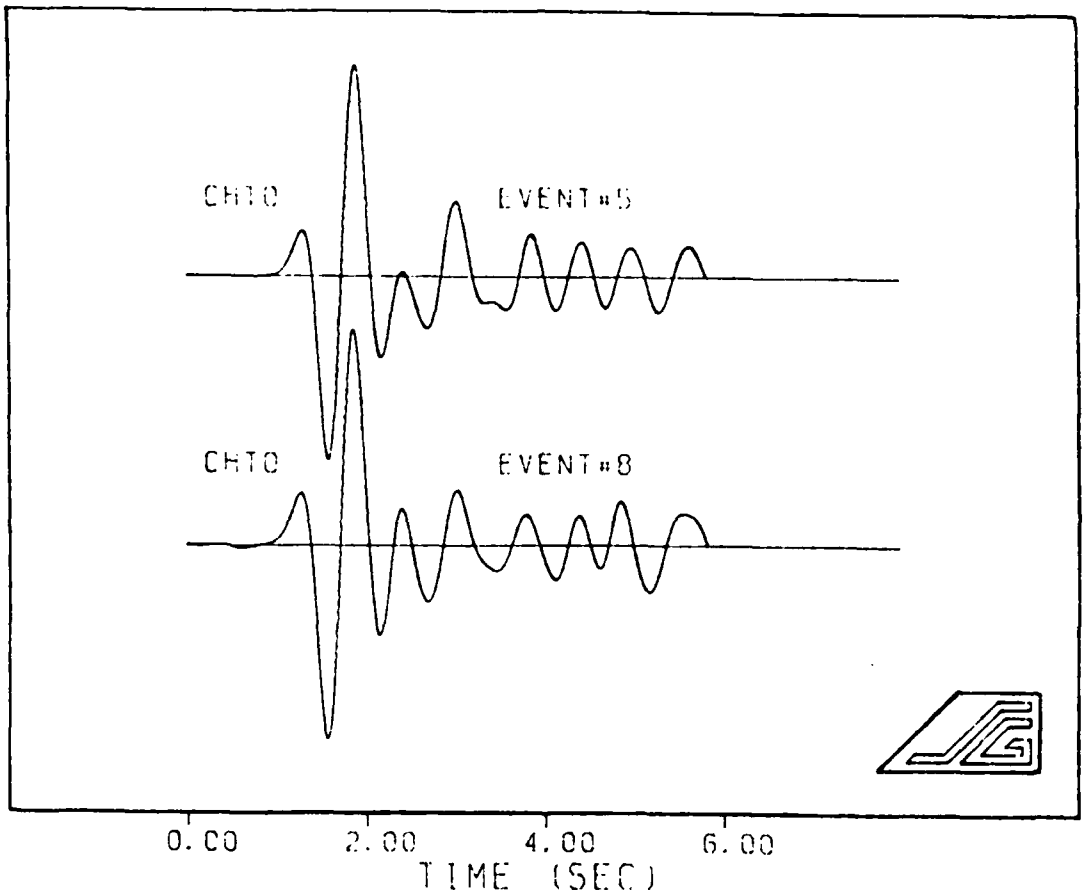

Figure 15:

Event seismograms 5 and 8 are shown above for station CHTO. These two events from Eastern Kazakh have almost identical waveshape even out to 6 seconds. They are however, very different from events 6 and 7 in both pulse width and second trough depth.

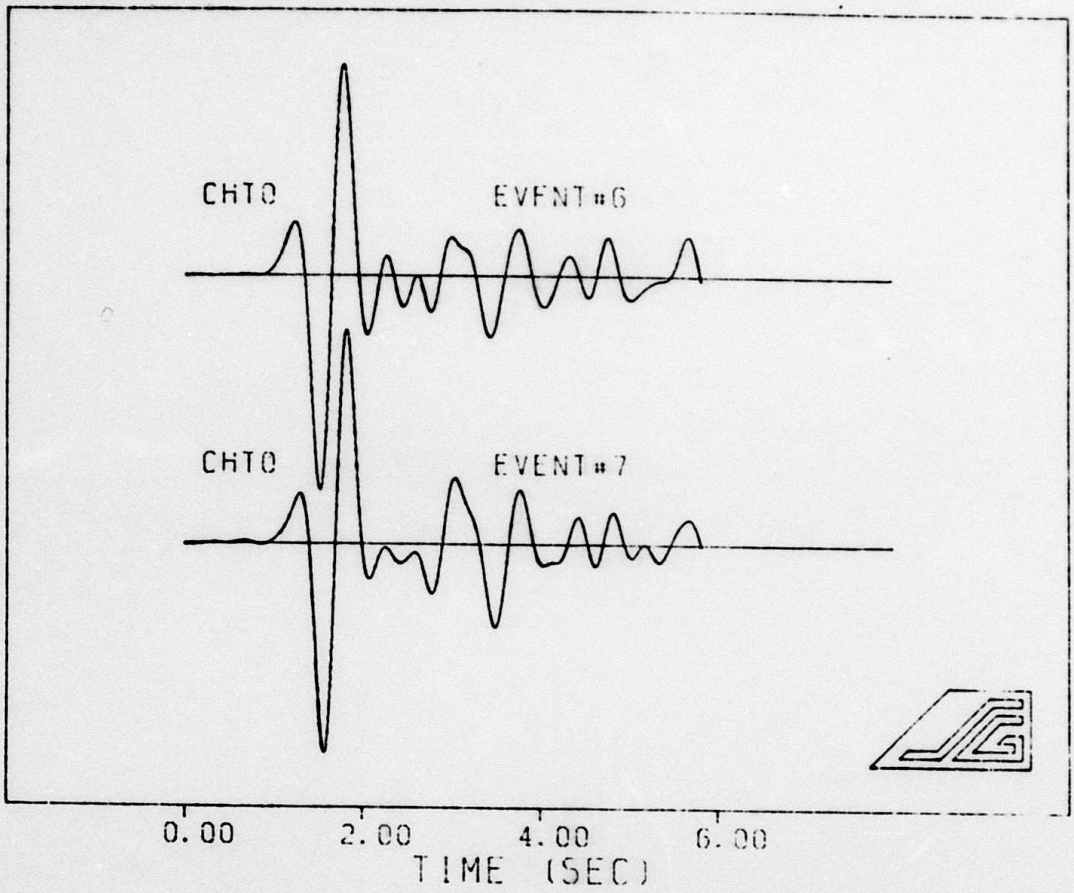

Figure 16. Event seismograms 6 and 7 are shown above for station CHTO. Both events occurred in Eastern Kazakh and appear to be almost identical at this S.E. Azimuth. The seismograms have a narrow width and a shallow second trough which was uncharacteristic of our other data.

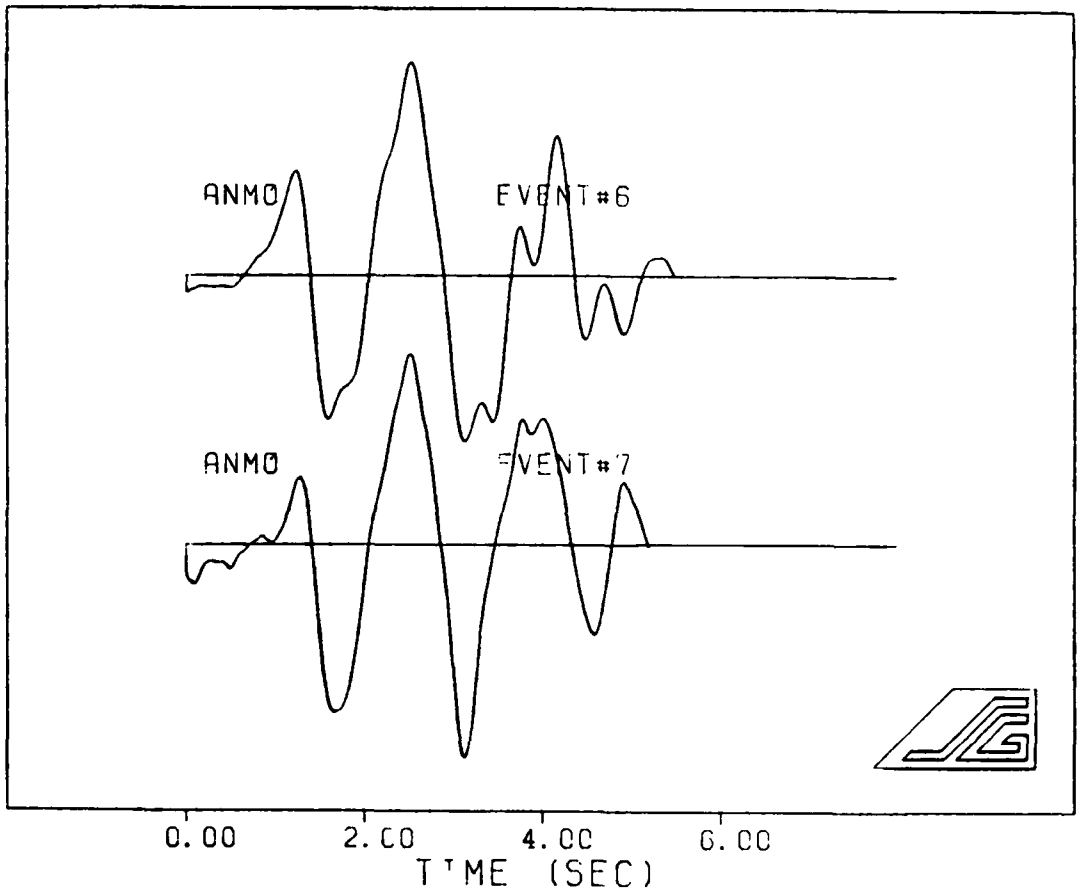

Figure 17. Event seismograms 6 and 7 are shown above for station ANMO. Both events occurred in Eastern Kazakh. Unlike the CHTO seismograms for the same events, these waveforms are noticably different in relative peak heights shape. This may be an indication of an azimuthally dependent source.

stable estimates of amplitude and delay time could be achieved by re-parameterizing the inversion scheme to solve for the differences and sums of those parameters and then employing a weighted regression to determine best estimates of the parameters themselves. This is the approach we have adopted in our present analysis.

Having once inverted the observed seismograms for the difference parameters, the best estimates of the absolute amplitudes and delays were obtained by solving the system of equations expressed by:

$$\underline{\rho}\ \underline{c}\ \underline{x} = \underline{\rho}\ \underline{b}$$

where

$$\underline{b} = \text{data column vector} = \begin{bmatrix} \Delta_{12} \\ \Delta_{13} \\ \vdots \\ \Sigma_{12} \\ \Sigma_{13} \end{bmatrix},$$

$$\underline{x} = \text{best estimate vector} = \begin{bmatrix} \tilde{A}_1 \\ \tilde{A}_2 \\ \vdots \\ \tilde{A}_N \end{bmatrix} \text{ or } \begin{bmatrix} \tilde{T}_1 \\ \tilde{T}_2 \\ \vdots \\ \tilde{T}_N \end{bmatrix},$$

$\underline{c}$ = a basis operator matrix which maps $\underline{x}$ into $\underline{b}$, and

$\underline{\rho}$ = a weighting vector

Δ_{ij} is the parameter difference between events i and j, Σ_{ij} is the parameter sum between events i and j; $\tilde{A}_1$ and $\tilde{T}_i$ are the best estimates of A_i and T_i respectively.

The weighting factors are proportional to the reciprocal of the variance. As a consequence, the differences (Δ_{ij}) are weighted more heavily than the sums (Σ_{ij}).

The errors from this approach may be determined by the weighted standard deviations. Fifty percent error bounds are then given by:

$$\varepsilon_A = .67 \quad \frac{\Sigma\rho(A-\tilde{A})^2}{(N-1)\Sigma\rho} \quad \text{, and}$$

$$\varepsilon_T = .67 \quad \frac{\Sigma\rho(T-\tilde{T})^2}{(N-1)\Sigma\rho}$$

Reduction of relative direct P data ($S = c_i/c_j$) for each inversion sum is done in the same manner except S is first linearized using the equation:

$$S_{ij} = \ln (c_i/c_j) = \ln c_i - \ln c_j$$

Best estimates of $\ln c_i$, expressed as $\ln \tilde{c}i$ are obtained by using the weighting scheme discussed above. Since S_{ij} is a relative measure, we need a relative error estimate. The error in S_{ij} for event i relative to event j may be expressed as:

$$\varepsilon = \pm(S_{ij} - \tilde{S}_{ij}) = S_{ij} \quad (1 - e^{\pm R_{ij}})$$

Where R_{ij} is the residual defined by the matrix equation:

$$\underline{R} = \underline{b} - \underline{C}\ \underline{x}$$

This error estimate relative to event j includes random and small systematic components. Large scale mismodeling due to bias or extra arrivals cannot be resolved in this manner.

In our experiments, two sets of results were obtained from the available data. In the first stage, only station CHTO was employed. Difficulties with parameter resolution were encountered for some data pairs, however, which complicated the interpretation of the results. The problem was corrected by adding additional stations to the inversion. Better resolution could also be obtained by adding another seismogram to the data base. The second set of results were obtained from 2 or 3 station inversions and are considered to be more reliable.

Table 1 lists the second set of reduced pP amplitudes and arrival times for each event, with 50% error bounds as derived from the error estimation methodology outlined above. Figure 18 is a graph of the results of the second round of calculations using both stations plotting amplitude vs. arrival time (and including calculated error bounds). Also plotted are the single station results (indicated by

Figure 18. Inversion results, giving effective pP amplitudes and delay times relative to direct arrival. Events divide into two populations by pP amplitude. Relative solutions for large pP events show little change between one and two station inversions, while small pP events show larger changes. Seismograms shown are comparison of data with synthetics for CHTO. Synthetics contain inversion solutions for pP time and amplitude, von Seggern-Blanford time function with k=10 B=1 and for CHTO.

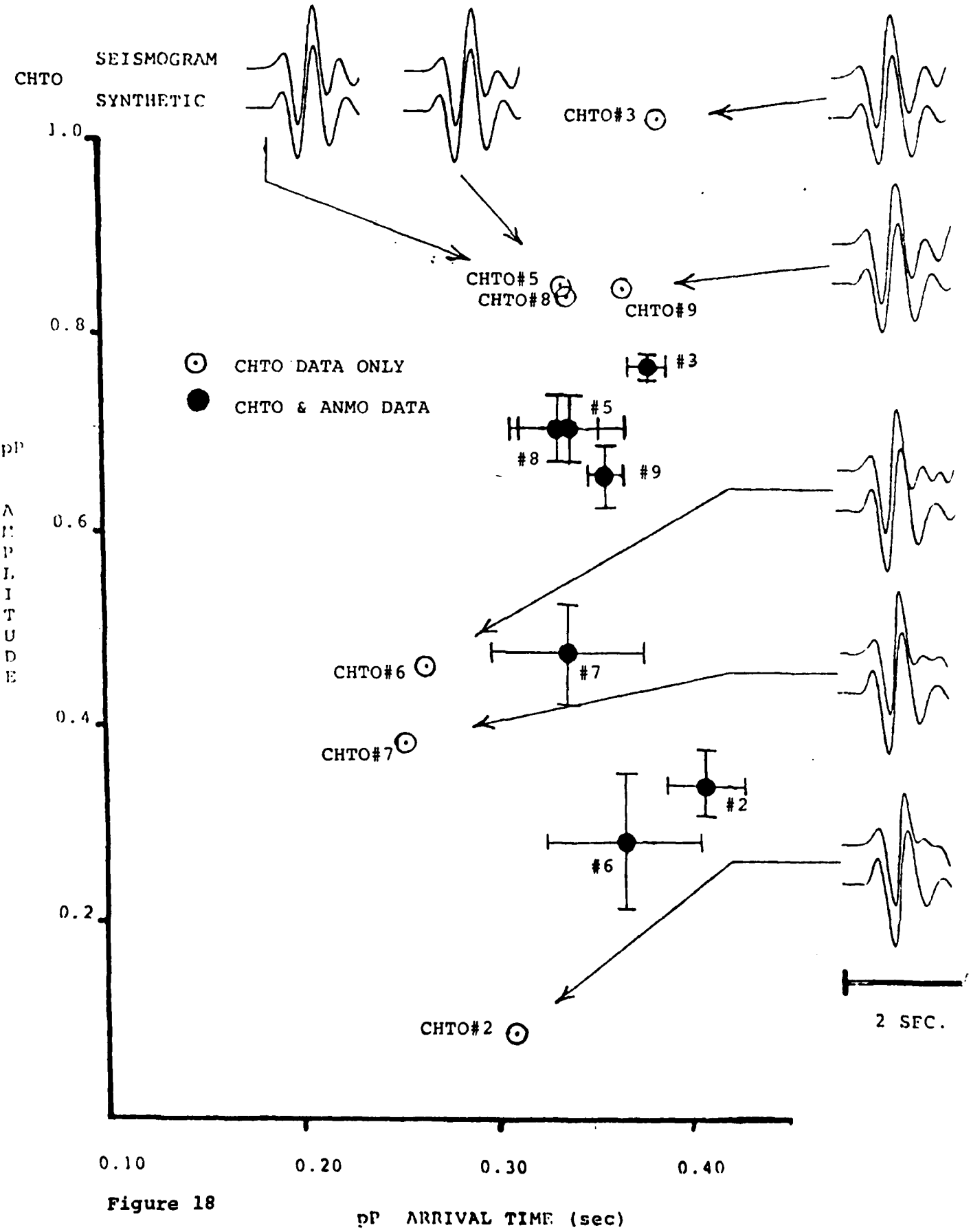
CHTO
SEISMOGRAM
SYNTHETIC
CHTO#3
CHTO#5
CHTO#8
CHTO#9
CHTO DATA ONLY
CHTO & ANMO DATA
#3
#5
#8
#9
#7
CHTO#6
CHTO#7
#2
#6
CHTO#2
2 SEC.
1.0
0.8
0.6
0.4
0.2
pP AMPLITUDE
0.10
0.20
0.30
0.40
pP ARRIVAL TIME (sec)

Figure 18

small circles). No error bounds were computed for the single station-derived model parameters.

A comparison of these two sets of results illustrates several notable points. In both sets of results two populations of events are evident. The first population, consisting of events 3, 5, 8 and 9, have a large (∿.7-.9) pP arrival. Differences between pP amplitudes and arrival times among these events are nearly identical for the one station and two station inversions. There is some change in absolute pP amplitude between the one and two station results. This is probably just a reflection of the fact that absolute pP amplitudes are much less well constrained by the relative waveform inversion than are relative pP amplitudes. Some possibility does exist, however, that the overall shift in pP amplitude is due to systematic azimuthal variation either in pP amplitude or in amplitude of an additional, unmodeled arrival.

The second population, consisting of events 2, 6, and 7 has pP amplitudes considerably smaller than expected from linear elastic theory. We note that both pP amplitudes and times change for tese events between the one and two station inversions, not only in an absolute sense but relative to other events as well. It is to be expected, perhaps, that arrival times will be poorly constrained for small arrivals (for zero amplitude the arrival time is totally unconstrained), and this result in in fact observed in the model variance matrices for the small pP population. The changes

in pP amplitud between the one and two event inversions, however, cannot be so easily explained away. Nor can the fact that events 6 and 7 are virtually identical at CHTO, but show more substantial differences at ANMO. This suggests either the presence of a second, probably positive, arrival with different azimuthal behavior for each of these events, or that whatever effect suppresses pP for these events shows substantial azimuthal variation. The consistency of relative times and amplitudes in the first population leads us to favor the second explanation, although considerably more work is clearly required in this area.

By design, the relative waveform inversion technique explicitly accounts for the interference of secondary arrivals when determining overall signal amplitude. Hence, such amplitude determinations may be more consistent than such standard measures of signal level as m_b or the amplitude of selected half-cycles of the short period waveform. In order to evaluate this effect, the relative amplitudes of the direct phases, as determined by the relative waveform inversion, have been compared to measurements of the A-phase (first peak), B-phase (first peak to first trough) and C-phase (first trough to second peak) measured amplitudes of all events with respect to event #7. Figures 19 and 20 plot the results of these comparisons for stations CHTO and ANMO respectively. A fairly good consistency is achieved at station CHTO but the near-receiver complexity at ANMO induces large scatter in the measured amplitudes. Only the

Figure 19. Comparison of inversion amplitude with other amplitude measures for all events at station CHTO. Simplicity of receiver function and good signal to noise ratio give reasonably consistent results for all measures used. All measurements referenced to event #7.

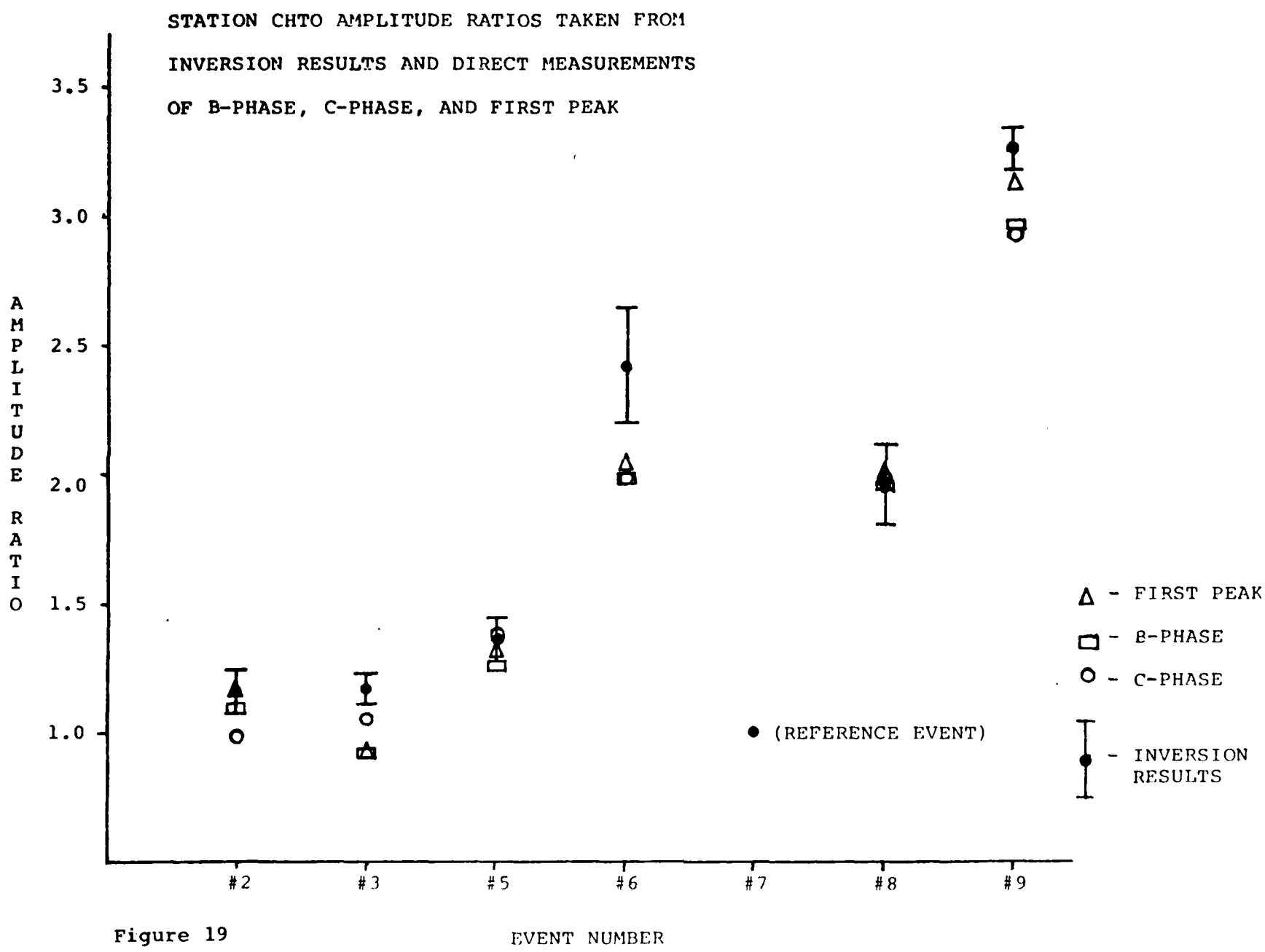
STATION CHTO AMPLITUDE RATIOS TAKEN FROM
INVERSION RESULTS AND DIRECT MEASUREMENTS
OF B-PHASE, C-PHASE, AND FIRST PEAK
AMPLITUDE RATIO
3.5
3.0
2.5
2.0
1.5
1.0
#2
#3
#5
#6
#7
#8
#9
EVENT NUMBER
● (REFERENCE EVENT)
- FIRST PEAK
- B-PHASE
- C-PHASE
- INVERSION RESULTS

Figure 19

Figure 20. Comparison of inversion amplitudes with other amplitudes measures for ANMO. Inversion results are most consistent with C-amplitudes. Various measures give different relative amplitude due to receiver function complications and noise.

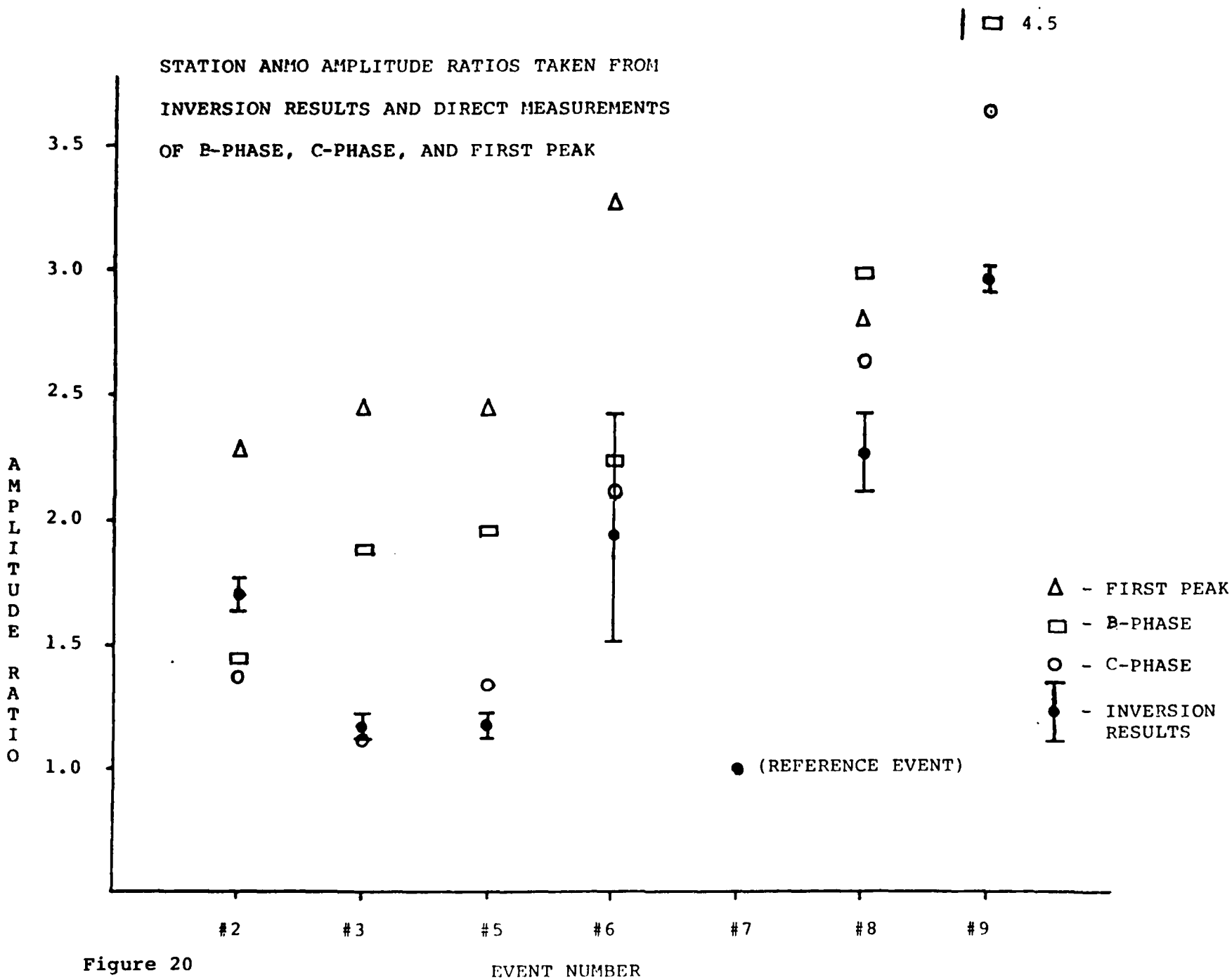
STATION ANMO AMPLITUDE RATIOS TAKEN FROM
INVERSION RESULTS AND DIRECT MEASUREMENTS
OF B-PHASE, C-PHASE, AND FIRST PEAK
AMPLITUDE RATIO
3.5
3.0
2.5
2.0
1.5
1.0
4.5
#2
#3
#5
#6
#7
#8
#9
EVENT NUMBER
(REFERENCE EVENT)
- FIRST PEAK
- B-PHASE
- C-PHASE
- INVERSION RESULTS

Figure 20

B-phase measurements at ANMO show something approaching a stable estimate. Finally, a comparison was made between the final inversion amplitudes ratios and the m_b amplitude ratios as reported in the Preliminary Determination of Epicenters complied by the U.S.G.S. We note at this time that PDE magnitude determinations often show errors of a few tenths of m_b units. Results of this comparison are shown in Figure 21, with both sets of amplitudes referenced to event #7. It is interesting to note that for events with large pP arrivals, m_b based amplitude determinations show these events to be much larger compared to event #7 than do the inversion results. This effect is not observed for the small pP population. A comparison of the inversion results with a more carefully done m_b study, presented in Part II of this report, shows the effect much more strikingly. Results of this study indicate that the bias in relative yield estimation between events having small and large pP arrivals can reach 40-50%, with the amplitude of the event with large pP being overestimated by m_b relative to the event with small pP.

Figure 21. Comparison of source amplitude ratios as determined by inversion and by M_b. Magnitude are from P.D.E. All events are referenced to event #7.

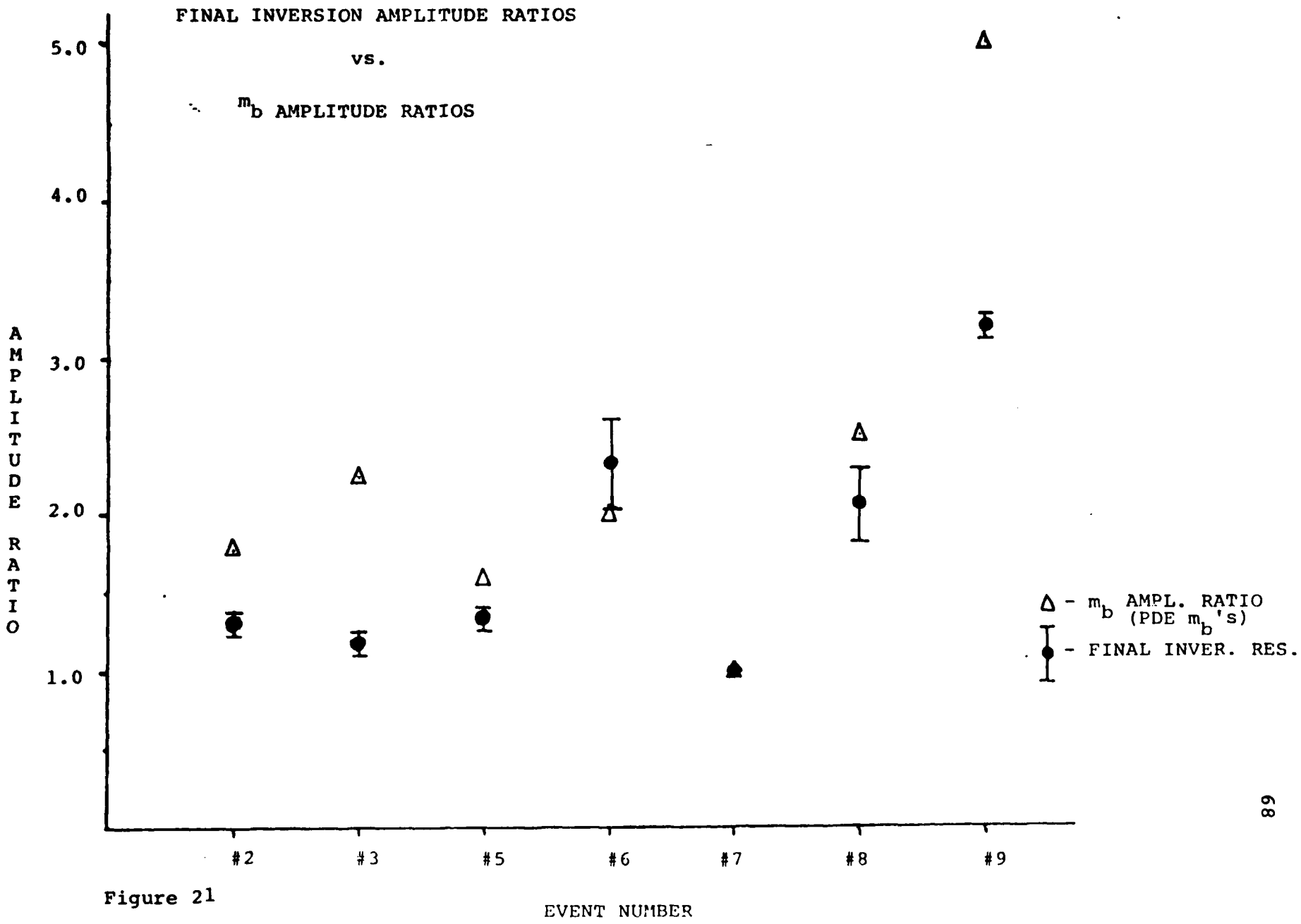
FINAL INVERSION AMPLITUDE RATIOS
vs.
m_b AMPLITUDE RATIOS
AMPLITUDE RATIO
5.0
4.0
3.0
2.0
1.0
#2
#3
#5
#6
#7
#8
#9
EVENT NUMBER
Δ - m_b AMPL. RATIO (PDE m_b's)
- FINAL INVER. RES.

Figure 21

V. CONCLUSIONS

The application of the relative waveform inversion technique thus far has clearly demonstrated several important features. First, it is possible to obtain well-resolved, stable estimates of relative event size, pP amplitude, and pP delay times from relatively sparse data sets and if necessary, from noisy or complex observations. Moreover, the biasing effects of fairly small changes in pP amplitude and delay time have been demonstrated on conventional yield estimation methodologies. This biasing seems generally to result in over-estimates (from m_b-type measures) of the yield of underground explosions of events with large pP.

This technique shows great promise in yield estimation and depth estimates of buried explosions, but clearly substantially more research efforts are required. The data base examined to date represents a relatively small number of events, azimuths from source to receiver, and stations. A more exhaustive testing program should be undertaken in order to fully test the procedure as well as provide a basis for any decision to incorporate this kind of analysis into formal monitoring procedures. Further research is alo necessary on the incorporation of relative waveform methods with absolute waveform methods to obtain even more accurate absolute amplitude and delay time measurements.

REFERENCES

Bache, T.C., S.M. Day, and J.M. Savino, Automated magnitude measures, earthquake source monitoring, VME discriminant testing and summary of current research, Quarterly Tech. Report SSS-R-79-3933, Systems, Science and Software, La Jolla, California, 1979.

Blandford, R.R., M.F. Tillman, and D.P. Racine, Empirical m_b - yield relations, SDAC-TR-76-14, Teledyne Geotech, Alexandria, VA., 2977.

Burkick, L.J. and D.V. Helmberger, Time functions appropriate for deep earthquakes, Bull. Seism. Soc. Am., 64, 1419-1428, 1974.

Burdick, L.J., t* for S waves with a continental ray path, Bull. Seism. Soc. Am., 68, p. 1013, 1978.

Burdick, L.J. and D.V. Helmberger, Time funtions appropriate for nuclear explosions, Bull. Seism. Soc. Am., 69, 957-973, 1979.

Haskell, N.A., Analytic approximation for the elastic radiation from a contained underground explosion, J. Geophys. Res., 72, 2583-2587, 1967.

Mellman, G.R., S.K. Kaufman, G.M. Lundquist, D.M. Hadley, R. S. Hart and C. A. Salvado, Comparisons of predicted far-field seismograms with observations of selected underground explosions, Sierra Geophysics, Inc. Report SGI-R-80-032, 1980.

Mellman, G.R., A method of body-wave waveform inversion for the determination of earth structure, Geophys. J. R. astr. Soc., 62, 481-504, 1980.

Perl, N. and J. Trulio, Effects of burial depth in seismic signals, Pacific Sierra Research Report #815, 1979.

von Seggern, D.H. and R.R. Blandford, Source time functions and spectra for underground nuclear explosions, Geophys. J. R. Astr. Soc., 31, p. 83, 1972.

APPENDIX

Partial derivatives for two seismogram relative waveform inversion

The source model for the two seismogram case is given by

$$S_1 = 1/c \quad \left(\delta(t) - a_1\, \delta(t-\tau_1)\right)$$
$$S_2 = c \quad \left(\delta(t+\tau_o) - a_2\, \delta\,(t+\tau_o-\tau_2)\right) \qquad \text{(A.1)}$$

The error function is given by

$$e = (f_1 * S_2 - S_1 * f_2) * W'$$
$$= F_1 * S_2 - S_1 * F_2 \quad \text{where} \qquad \text{(A.2)}$$
$$F_i = f_i * W'$$

Then, defining m_j, the model vector, by

$$\underline{m} = (a_1, a_2, c, \tau_o, \tau_1, \tau_2)$$

Letting e_i be the jth time point in the time series e we find

$$A_{ij} = \frac{\partial e_i}{\partial m_j} \qquad \text{is given by}$$

$$\frac{\partial e_i}{\partial a_1} = \frac{1}{c} F_2 (t_i - \tau_1)$$

$$\frac{\partial e_i}{\partial a_2} = cF_1(t_i + \tau_o - \tau_2)$$

$$\frac{\partial e_i}{\partial c} = F_1 (t_i + \tau_o) - a_2 F_1 (t_i - \tau_o - \tau_2) + \frac{1}{c^2} F_2 (t_i)$$

$$- \frac{a_1}{c^2} F_2 (t_i - \tau_1)$$

$$\frac{\partial e_i}{\partial \tau_o} = cF'_1 (t_i + \tau_o) - a_2 cF'_1 (t_i + \tau_o - \tau_2)$$

$$\frac{\partial e_i}{\partial \tau_1} = - \frac{a_1}{c} F'_2 (t_j - \tau_1)$$

$$\frac{\partial e_i}{\partial \tau_2} = a_2 c F'_1 (t_i + \tau_o - \tau_2)$$